Manuscript # acp-2016-1032

Responses to Reviewer #1

The authors used the CESM model with a source-tagging method to quantify the source attributions for BC direct radiative forcing (DRF) and concentration as well as polluted events. They found that in addition to regional emissions within China, emissions outside China also contribute to a large portion of BC DRF over China. This study could improve the understanding on BC pollution in China and provide implications for policy makers. Before this manuscript can be considered for publication, I have a few comments that need to be addressed by the authors.

1. One critical factor influencing BC direct radiative effect is its optical properties (absorption and extinction cross section, asymmetry factor, and single scattering albedo). Recent studies (e.g., He et al. 2015, 2016b) showed that BC optical properties vary significantly (by up to more than a factor of two) due to different coating structures and aging stages during BC aging process, which further affects direct radiative effect. (1) Could the authors add some discussions on this aspect with reference to these recent studies, for example, potential uncertainty in their results caused by this factor? (2) Could this variation in BC optical properties due to coating structures contribute to the model biases in BC AAOD simulations as discussed in the first paragraph of Section 3.2? (3) It would be helpful if the authors could add more details on how the MAM3 model computes BC optical properties. For example, does it assume a core-shell structure for internally mixed BC?

References:

He, C., et al. : Variation of the radiative properties during black carbon aging: theoretical and experimental intercomparison, Atmos. Chem. Phys., 15, 11967-11980, doi:10.5194/acp-15-11967-2015, 2015.

He, C., et al. : Intercomparison of the GOS approach, superposition T-matrix method, and laboratory measurements for black carbon optical properties during aging, J. Quant. Spectrosc. Radiat. Transf., 184, 287–296, doi:10.1016/j.jqsrt.2016.08.004, 2016b.

Response:

(1) Thanks for the suggestion. We have added discussions of the influence of aging processes on BC optical properties to the Conclusions and Discussions section, along with the references provided by the referee, as “BC aging in the atmosphere is important for BC concentration and its optical properties, which transforms BC from hydrophobic aggregates to hydrophilic particles coated with soluble materials. He et al. (2015, 2016a) found that BC optical properties varied by a factor of two or more due to different coating structures during BC aging process based on their theoretical and experimental intercomparison. Oshima et al. (2009) and He et al. (2016b) pointed out that the use of various microphysical BC aging schemes could significantly improve simulations of BC concentrations compared to

the simplified aging parameterizations. Liu et al. (2012) also reported that the wet removal rate of BC simulated in standard CAM5 is 60% higher than AeroCom multi-model mean due to the rapid or instantaneous aging of BC. H. Wang et al. (2013) showed that the explicit treatment of BC aging process with slow aging assumptions in CAM5 could significantly increase BC lifetime and the efficiency of BC long-range transport. In the three-mode aerosol module (MAM3) of CAM5 used in this study, the aging process of BC is neglected by assuming the immediate internal mixing of BC with other aerosol species in the same mode. This assumption could lead to an overestimation of wet removal of BC and, therefore, an underestimation of BC concentrations, absorption optical depth (Fig. 3) and direct radiative forcing. In addition, the internally-mixed optical treatment in CAM5 could also cause bias in BC absorption calculation. However, H. Wang et al. (2014) examined source-receptor relationships for BC under the different BC aging assumptions and found that the quantitative source attributions varied slightly while the qualitative source-receptor relationships still hold. Therefore, although the magnitude of simulated BC and its optical properties could be underestimated due to the instantaneous aging of BC and uncertainty in coating structures, we expect that the aging treatment in MAM3 of CAM5 should not influence the qualitative source attributions examined in this study."

(2) We agree that uncertainties in BC optical properties due to coating structures and/or aging could contribute to model biases in simulated BC concentrations and AAOD. We have added this statement in the discussion section. Please see the revisions above.

(3) In the MAM3 aerosol module of CAM5 used in this study, the aging process of BC is neglected by assuming an instantaneous mixing of BC with other aerosol species in the same accumulation mode, which has been added in the discussion section. We also add a more detailed description of the calculation of aerosol optical properties in the Methods section, as "Aerosol optical properties for each mode are parameterized according to Ghan and Zaveri (2007). Refractive indices for aerosols are taken from the OPAC (optical properties for aerosols and clouds) software package (Koepke and Schult, 1998), but for BC at solar wavelengths the values are updated from Bond and Bergstrom (2006)."

2. For BC emissions, a number of global and regional emission inventories have been developed, which showed large uncertainties and differences among each other (e.g., Fig. 4 in Wang et al., 2014). It would be helpful if the authors could discuss the uncertainty associated with the emission inventory used in this study and how this inventory compares with previous ones for both inside and outside China, since the authors pointed out that emissions outside China also contribute a lot to BC DRF in China.

Reference:

Wang, R., et al. : Trend in Global Black Carbon Emissions from 1960 to 2007, Environ. Sci. Technol., 48, 6780−6787, doi: 10.1021/es5021422, 2014.

Response:

Uncertainty in China BC emissions has been estimated as –43% to 93% by Lu et al. (2011), –50% to 164% by Qin and Xie (2012), ±176% by Kurokawa et al. (2013), and –28 to 126% by Zhao et al. (2013). The BC emissions estimates used here for China in 2010 are 40% higher than those of Zhao et al. (2013) and Lu et al. (2011) and 30% higher than Klimont et al. (2016), in large part due to a higher estimate of BC emissions from coal coke production. Emissions from coke production are particularly uncertain given that "there are no measurements for $PM_{2.5}$ and BC emissions" (Huo et al. 2012) available to guide inventory estimates. Total rest of the world emissions other than China, which appear to be a major contributor to burdens over western regions, are within 1% of those from Klimont et al. (2016). We have added these discussions in Conclusions and discussions section.

We have added Table S1 to compare the anthropogenic emissions used in this study with emissions from some previous studies. The anthropogenic emissions of BC in China in 2010–2014 are larger than those used in the previous studies for earlier years, partly as a result of a higher estimate of BC emissions from coal coking production. The higher emissions likely lead to higher concentrations and direct radiative forcing, and source contributions of BC in China, compared to the values reported in these studies. We have added these descriptions in the Methods section.

We also revised Fig. 1 to include BC emissions from outside China. Emissions at regional scale are summarized here instead of Country level because the model revolution is a bit course to characterize emissions by countries. Total BC emissions from neighboring regions including rest of East Asia (REA, with China excluded), South Asia (SAS), Southeast Asia (SEA), and Russia/Belarussia/Ukraine (RBU) are shown in Figure 1c. These source regions outside China are consistent with source regions defined in the second phase of Hemispheric Transport of Air Pollution (HTAP2). South Asia and Southeast Asia have relatively high emissions. They may dominate the contribution to concentrations and direct radiative forcing of BC in China, especially southern and western China, from foreign sources through long-range transport. We have also added these in the Methods section. We did not compare the emissions outside China with other studies, which is beyond the scope of this study. However, the comparison of CEDS emissions with other emission inventories can be found in Hoesly et al. (2017), which includes detailed information of the CEDS emissions and will be submit very soon.

Table S1. Comparison of CEDS annual mean anthropogenic BC emissions in China with those used in other studies

	Year	Anthropogenic emission in China (Gg/yr)
CEDS (Hoesly et al., 2016; this study)	2010–2014	2467
MIX (Li et al., 2017)	2010	1765
HTAP V2.2 (Janssens-Maenhout et al., 2015)	2010	1741
Lu et al. (2011)	2010	1751
Qin and Xie (2012)	2009	1764
Wang et al. (2012)	2007	1879
INTEX-B (Zhang et al., 2009)	2006	1811

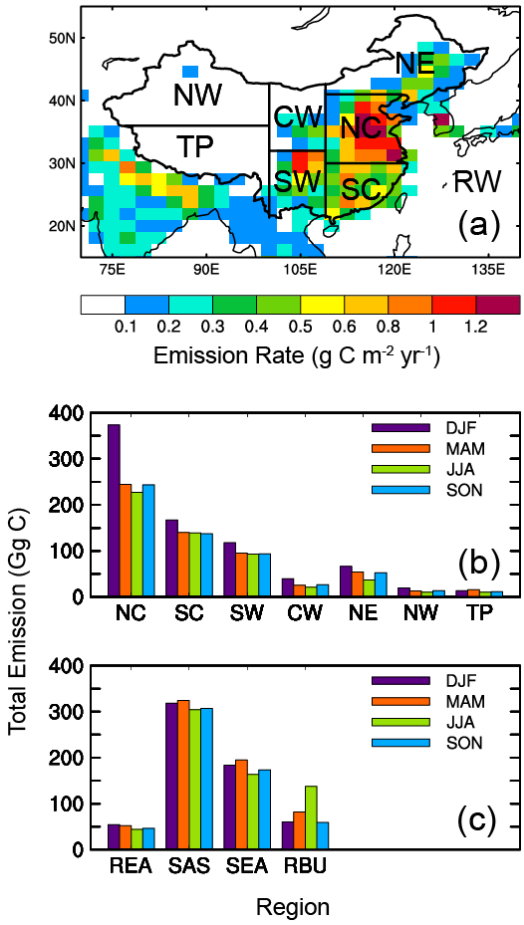

Figure 1. (a) Spatial distribution of annual mean total emissions (anthropogenic plus biomass burning, units: g C m^{-2} yr^{-1}) of black carbon (BC) averaged over 2010–2014. The geographical BC source regions are selected as North China (NC, 109°E–east boundary, 30°–41°N), South China (SC, 109°E–east boundary, south boundary–30°N), Southwest China (SW, 100°–109°N, south boundary–32°N), Central-West China (CW, 100°–109°N, 32°N–north boundary), Northeast China (NE, 109°E–east boundary, 41°N–north boundary), Northwest China (NW, west boundary–100°E, 36°N–north boundary), and Tibetan Plateau (TP, west boundary–100°E, south boundary–36°N) in China and regions outside of China (RW, rest of the world). (b) Seasonal mean total emissions (units: Gg C, Gg = 10^9g) of BC from the seven BC source regions in China and (c) emissions from rest of East Asia (REA, with China excluded), South Asia (SAS), Southeast Asia (SEA), and Russia/Belarussia/Ukraine (RBU).

3. Another important factor affecting BC simulations is aging process, which directly alters BC wet scavenging and lifetime. As pointed out by some recent studies (e.g., Oshima et al., 2009; He et al., 2016a), applying microphysical BC aging schemes could significantly improve simulations of BC concentrations compared with simplified aging parameterizations. (1) Could the authors briefly describe how BC aging is treated/computed in their model? (2) It would be helpful if the authors could briefly discuss the BC aging effect on their results with reference to these recent studies. (3) The authors mentioned in Lines 255–256 that model biases in BC concentration over China is likely due to inaccurate emissions and wet scavenging. Could this bias also be caused by model uncertainty related to BC aging? Some discussions would be useful.

reference:

He, C., Li, Q., Liou, K.-N., Qi, L., Tao, S., and Schwarz, J. P.: Microphysics-based black carbon aging in a global CTM: constraints from HIPPO observations and implications for global black carbon budget, Atmos. Chem. Phys., 16, 3077-3098, doi:10.5194/acp-16-3077-2016, 2016a.

Oshima, N., et al. : Aging of black carbon in outflow from anthropogenic sources using a mixing state resolved model: Model development and evaluation, J. Geophys. Res., 114, D06210, doi:10.1029/2008JD010680, 2009.

Response:

(1) Thanks for the suggestion. We had now added more description of the BC aging treatment and related discussions to the paper. Please see the response to comment #1 above.

(2) Following the referee's suggestion, we had now added more discussions in this regard. Please see the response to comment #1 above.

(3) Yes, the overestimation of wet scavenging is partly caused by the assumption of instantaneous aging of BC in the model. We have added the message to the manuscript, as "Larger wet removal rate and shorter lifetime of aerosols along with the instantaneous aging of BC in the MAM3 can also lead to the lower concentrations of BC (e.g., Wang et al., 2011; Liu et al., 2012; H. Wang et al., 2013; Kristiansen et al., 2016)." and in discussion section as "This assumption could lead to an overestimation of wet removal of BC and, therefore, an underestimation of BC concentrations, absorption optical depth (Fig. 3) and direct radiative forcing."

4. The authors derived BC AAOD from AERONET observations by using the method in Bond et al. (2013). However, a recent study by Schuster et al. (2016) pointed out some weaknesses and problems related to the Bond et al. (2013) method. Could the author briefly discuss this issue? How would this affect the results in this study?

Reference:
Schuster, G. L., et al. : Remote sensing of soot carbon – Part 2: Understanding the absorption Ångström exponent, Atmos. Chem. Phys., 16, 1587–1602, doi:10.5194/acp-16-1587-2016, 2016.

Response:

We have included a discussion of this caveat associated with the BC AAOD comparison, as "Note that, the observed AAOD of BC is derived from AERONET measurements using the absorption Ångström exponent. A recent study (Schuster et al., 2016) reported that absorption Ångström exponent is not a robust parameter for separating out carbonaceous absorption in the AERONET database, which could cause biases in the AAOD estimates."

References:

He, C., Liou, K.-N., Takano, Y., Zhang, R., Levy Zamora, M., Yang, P., Li, Q., and Leung, L. R.: Variation of the radiative properties during black carbon aging: theoretical and experimental intercomparison, Atmos. Chem. Phys., 15, 11967-11980, doi:10.5194/acp-15-11967-2015, 2015.

He, C., Takano, Y., Liou, K.-N., Yang, P., Li, Q., and Mackowski, D. W.: Intercomparison of the GOS approach, superposition T- matrix method, and laboratory measurements for black carbon optical properties during aging, J. Quant. Spectrosc. Ra., 184, 287–296, doi:10.1016/j.jqsrt.2016.08.004, 2016a.

Kristiansen, N. I., Stohl, A., Olivié, D. J. L., Croft, B., Søvde, O. A., Klein, H., Christoudias, T., Kunkel, D., Leadbetter, S. J., Lee, Y. H., Zhang, K., Tsigaridis,

K., Bergman, T., Evangeliou, N., Wang, H., Ma, P.-L., Easter, R. C., Rasch, P. J., Liu, X., Pitari, G., Di Genova, G., Zhao, S. Y., Balkanski, Y., Bauer, S. E., Faluvegi, G. S., Kokkola, H., Martin, R. V., Pierce, J. R., Schulz, M., Shindell, D., Tost, H., and Zhang, H.: Evaluation of observed and modelled aerosol lifetimes using radioactive tracers of opportunity and an ensemble of 19 global models, Atmos. Chem. Phys., 16, 3525-3561, doi:10.5194/acp-16-3525-2016, 2016.

Liu, X., et al. (2012), Toward a minimal representation of aerosols in climate models: Description and evaluation in the Community Atmosphere Model CAM5, Geosci. Model Dev., 5, 709–739, doi:10.5194/gmd-5-709-2012.

Liu, X., Ma, P.-L., Wang, H., Tilmes, S., Singh, B., Easter, R. C., Ghan, S. J., and Rasch, P. J.: Description and evaluation of a new four-mode version of the Modal Aerosol Module (MAM4) within version 5.3 of the Community Atmosphere Model, Geosci. Model Dev., 9, 505-522, doi:10.5194/gmd-9-505-2016, 2016.

Wang, H., R. C. Easter, P. J. Rasch, M. Wang, X. Liu, S. J. Ghan, Y. Qian, J.-H. Yoon, P.-L. Ma, and V. Vinoj (2013), Sensitivity of remote aerosol distributions to representation of cloud-aerosol interactions in a global climate model, Geosci. Model Dev., 6, 765–782, doi:10.5194/gmd-6-765-2013.

Wang, H., P. J. Rasch, R. C. Easter, B. Singh, R. Zhang, P.-L. Ma, Y. Qian, S. J. Ghan, and N. Beagley (2014), Using an explicit emission tagging method in global modeling of source-receptor relationships for black carbon in the Arctic: Variations, sources, and transport pathways, J. Geophys. Res. Atmos., 119, 12,888–12,909, doi:10.1002/ 2014JD022297.

Ghan, S. J., and R. A. Zaveri (2007), Parameterization of optical properties for hydrated internally mixed aerosol, J. Geophys. Res., 112, D10201, doi:10.1029/2006JD007927.

Bond, T. C., and R. W. Bergstrom, Light absorption by carbonaceous particles: An investigative review, Aerosol. Sci. Technol., 40, 27–67, doi:10.1080/02786820500421521, 2006.

Koepke, M. H. P., and I. Schult, Optical properties of aerosols and clouds: The software package opac, Bull. Am. Meteorol. Soc., 79, 831–844, 1998, doi:10.1175/1520-0477(1998)079<0831:OPOAAC>2.0.CO;2.

Wang, M., S. Ghan, M. Ovchinnikov, X. Liu, R. Easter, E. Kassianov, Y. Qian, and H. Morrison (2011), Aerosol indirect effects in a multi-scale aerosol-climate model PNNL-MMF, Atmos. Chem. Phys., 11, 5431–5455, doi:10.5194/acp-11-5431-2011.

He, C., Li, Q., Liou, K.-N., Qi, L., Tao, S., and Schwarz, J. P.: Microphysics-based black carbon aging in a global CTM: constraints from HIPPO observations and implications for global black carbon budget, Atmos. Chem. Phys., 16, 3077-3098, doi:10.5194/acp-16-3077-2016, 2016b.

Oshima, N., M. Koike, Y. Zhang, Y. Kondo, N. Moteki, N. Takegawa, and Y. Miyazaki (2009), Aging of black carbon in outflow from anthropogenic sources using a mixing state resolved model: Model development and evaluation, J. Geophys. Res., 114, D06210, doi:10.1029/2008JD010680.

Schuster, G. L., Dubovik, O., Arola, A., Eck, T. F., and Holben, B. N.: Remote sensing of soot carbon – Part 2: Understanding the absorption Ångström exponent, Atmos. Chem. Phys., 16, 1587-1602, doi:10.5194/acp-16-1587-2016, 2016.

Kurokawa, J., Ohara, T., Morikawa, T., Hanayama, S., Janssens-Maenhout, G., Fukui, T., Kawashima, K. and Akimoto, H.: Emissions of air pollutants and greenhouse gases over Asian regions during 2000–2008: Regional Emission inventory in ASia (REAS) version 2, Atmospheric Chem. Phys., 13(21), 11019–11058, 2013.

Qin, Y. and Xie, S. D.: Spatial and temporal variation of anthropogenic black carbon emissions in China for the period 1980–2009, Atmos Chem Phys, 12(11), 4825–4841, doi:10.5194/acp-12-4825-2012, 2012.

Zhao, Y., Zhang, J. & Nielsen, C. P. 2013. The effects of recent control policies on trends in emissions of anthropogenic atmospheric pollutants and CO_2 in China. Atmos. Chem. Phys., 13, 487-508.

Lu, Z., Zhang, Q. & Streets, D. G. 2011. Sulfur dioxide and primary carbonaceous aerosol emissions in China and India, 1996–2010. Atmos. Chem. Phys., 11, 9839-9864.

Huo, H., Lei, Y., Zhang, Q., Zhao, L. & He, K. 2012. China's coke industry: Recent policies, technology shift, and implication for energy and the environment. Energy Policy, 51, 397-404.

Klimont, Z., Kupiainen, K., Heyes, C., Purohit, P., Cofala, J., Rafaj, P., Borken-Kleefeld, J. and Schöpp, W.: Global anthropogenic emissions of particulate matter including black carbon, Atmospheric Chem. Phys. Discuss., 1–72, doi:10.5194/acp-2016-880, 2016.

Manuscript # acp-2016-1032

Responses to Reviewer #2

Yang et al. investigated the BC source attributions (or more specifically, region attributions) in China with a source-tagging technique by employing a global climate model, NCAR's Community Earth System Model. They found out that BC emissions from local (inside China) and non-local (outside China) are both generally important contributions to air quality in different regions of China, BC outflow from East Asia and direct radiative forcings. Overall, this paper is a helpful addition to our community that attempts to improve our understanding of BC source-receptor relationship. This paper generally reads well and is within the scope of ACP. However, before it can be accepted for publication in ACP, I have several comments that need to be properly addressed.

Major comments:

An important part of this study was to quantify the BC source contributions to trans-boundary and trans-pacific transport. In terms of model performance evaluation, this study only validated model simulations with observed BC surface concentrations from CAWNET and AAOD from AERONET over China. We don't know the efficiency of BC outflow from East Asia. In this paper, it obviously missed the evaluations of model simulated vertical profiles of BC against aircraft campaign observations, e.g. A-FORCE and HIPPO, which should be employed to compare with model simulations.

Response:

Thanks for the suggestion. The simulated BC vertical profile in CAM5 has been extensively evaluated in many previous studies. Liu et al. (2012) compared the observed and simulated BC vertical profiles in the tropics, middle latitudes, and high latitudes from six aircraft campaigns: AVE Houston (NASA Houston Aura Validation Experiment), CR-AVE (NASA Costa Rica Aura Validation Experiment), TC4 (Tropical Composition, Cloud and Climate Coupling), CARB (NASA initiative in collaboration with California Air Resources Board), ARCTAS (NASA Arctic Research of the Composition of the Troposphere from Aircraft and Satellite), and ARCPAC (NOAA Aerosol, Radiation, and Cloud Processes affecting Arctic Climate), as well as BC vertical profiles over the Arctic Ocean and the remote Pacific Ocean during the HIPPO (HIAPER Pole-to-Pole Observations) campaign. They found that measured BC mixing ratios showed a strong gradient from the boundary layer to the free troposphere in the tropics, while modeled BC mixing ratios showed a smaller decrease with altitude in the free troposphere, thus overestimating observations above 500 hPa. Compared to HIPPO campaign, the CAM5 model captured the vertical variations of BC mixing ratio reasonably well in the SH high latitudes and NH

and SH mid-latitudes. However, modeled BC showed less vertical reduction in the tropics, thus significantly overestimating BC in the upper troposphere.

Wang et al. (2013) implemented in CAM5 a unified treatment of wet removal and vertical transport of aerosols by convection, which included an explicit secondary activation of aerosols being laterally entrained into convective clouds above cloud base. The comparisons between the new CAM5 simulated vertical profiles of BC mass mixing ratios and the HIPPO and the field campaign aircraft observations showed a substantial improvement in the simulation of BC in mid- and upper troposphere, where the excessive BC was significantly reduced. All of these key model improvements by Wang et al. (2013) have been included in the version of CAM5 being used in the present study. Therefore, we did not duplicate the evaluation of BC vertical profiles with HIPPO observation. We have now revised the description before model evaluation to make it clear, as "The simulations of aerosols, especially BC, using CAM5 have been extensively evaluated against observations including aerosol mass and number concentrations, vertical profiles, aerosol optical properties, aerosol deposition, and cloud-nucleating properties in several previous studies (e.g., Liu et al., 2012, 2016; H. Wang et al., 2013; Ma et al., 2013b; Jiao et al., 2014; Qian et al., 2014; R. Zhang et al., 2015a,b)."

In addition, as the referee suggested, we have added a comparison of the simulated BC vertical profile with A-FORCE measurements over East Asia (see Figure S2). The model successfully reproduces the vertical profile of BC. The bias is relatively small. We have also added a relevant discussion to the revised manuscript, as "Figure S2 compares the observed and simulated vertical profiles of BC concentrations in the East-Asian outflow region. The model successfully reproduces the vertical profile of BC that was measured in March–April 2009 during the A-FORCE field campaign and reported by Oshima et al. (2012)."

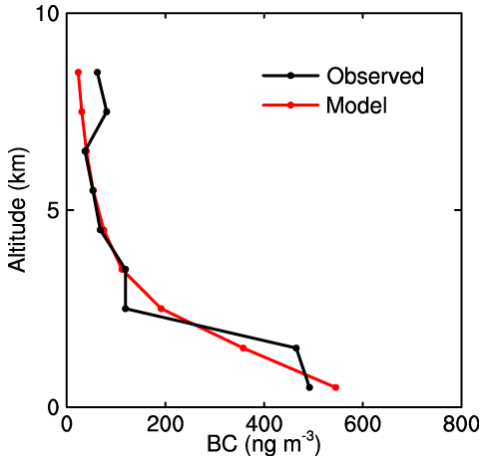

Figure S2. Observed and simulated mean vertical profiles of BC concentrations in the East-Asian outflow region. The observed BC profile is from the A-FORCE field

campaign conducted over the Yellow Sea, the East China Sea, and the western Pacific Ocean in March–April 2009 (Oshima et al., 2012).

Other minor comments:

Line 124: the reference Hoesly et al., 2016 is missing in the reference list.
Response:
The paper is still in preparation. A draft can be made available to referees upon request.

Line 162: A brief description of dry/wet deposition scheme for BC in CAM is lacking here, especially the wet scavenging and how it is improved following H. Wang et al. (2013).
Response:
Aerosol dry deposition velocities are calculated using the Zhang et al. (2001) parameterization. The wet deposition of aerosols in our CAM5 model includes in-cloud wet removal (i.e., activation of interstitial aerosols to cloud-borne particles followed by precipitation scavenging) and below-cloud wet removal (i.e., capture of interstitial aerosol particles by falling precipitation particles) for both stratiform and convective clouds. Aerosol activation is calculated with the parameterization of Abdul-Razzak and Ghan (2000) for stratiform cloud throughout the column and convective cloud at cloud base, while the secondary activation above convective cloud base has a simpler treatment with an assumed maximum supersaturation in convective updrafts (H. Wang et al., 2013). The unified treatment for convective transport and aerosol wet removal along with the explicit aerosol activation above convective cloud base was developed by H. Wang et al. (2013) and included in the CAM5 version being used in this study. As discussed in the response to the major comment, this implementation reduces the excessive BC aloft and better simulates observed BC concentrations in the mid- to upper-troposphere.
We have now added these descriptions to the Methods section.

Line 334-336: This sentence should be corrected as “AI derived from Total Ozone Mapping Spectrometer (TOMS) measurements also shows similar pattern as simulate AAOD (Fig. S2).”
Response:
Corrected.

Line 339-344: What’s the assumption here? Why the ratio of AAOD to AI should be the same between western and eastern China? What is the role of dust here in assisting the speculation?
Response:

Based on the comparison of AAOD between the model simulation and AERONET, we found that the model reproduced well the observed AAOD over eastern China. Therefore, we assume that the ratio of modeled AAOD and satellite AI (indicator for absorbing aerosols) is correct over eastern China. The AAOD/AI over eastern China is much larger than western China, suggesting that the ratio AAOD/AI is lower than the true value and AAOD or BC burden is likely underestimated in the model. Both AAOD and AI represent absorbing aerosols, the ratio of AAOD to AI may be different but similar between different regions in China. The difference in the ratio between eastern and western China is quite large, suggesting the existence of a significant bias. This is consistent with the contrast of biases in near-surface BC concentrations between the two regions (shown in Fig. 3). However, both BC and dust can contribute to AAOD and AI. Potential biases in the modeled dust could also lead to the inconsistence of AAOD/AI between eastern and western China.

We have revised the description to make it clear, as "If we assume that the simulated AAOD do not have large biases over eastern China based on the evaluation against observations shown above (Fig. 3b and Table S3), then this difference hints a possible underestimation of BC column burden in the model over the western regions. However, it is difficult to draw a firm conclusion, given the likely differential role of dust in eastern vs western China. This differential likely also contributes to AAOD biases in modeling dust and may also impact biases in the satellite derived AI values."

Line 424-426: I think BC emissions from SC are also important for the column burdens over continental China in some seasons (e.g. JJA and SON), which needs to be outlined as well.

Response:

Thanks for the suggestion. We have now added the SC contribution to column burden, as "Column burdens of BC averaged over continental China mainly originate from emissions in North China, South China and outside China, with relative contributions ranging from 31–42%, 16–24% and 14–31%, respectively."

Line 443: "Figure S4a" should be replaced with "Fig. S5a".

Response:

Corrected.

Line 443-463: It is helpful for the authors to make supplemental plots showing the anomalous winds during polluted days that favor the accumulation of pollutants over each region.

Response:

We did show in Fig. 8 the anomalous winds at 850 mb between polluted and normal days for each region during winter.

Line 505-509: Why the authors only choose the latitude range along longitude 150°E, not a domain covering East China Sea and West Pacific to quantitatively assess the

BC contributions from China and outside China, similar to that impact over West United States?

Response:

The outflow of aerosols, defined as the column-integrated aerosol flux or concentration along a vertical cross-section, is used to characterize the export of BC from East Asia. This calculation of outflow follows previous studies and thus is comparable to the results in these studies (Hadley et al., 2007; Matsui et al., 2013; Yang et al., 2015). In addition, using a region around 150°E does not change the values significantly (e.g., contribution from China changes from 53% for the outflow at150°E to 54% for an average over 145–155°E). We don't mean to assess the contributions from China and outside China to air quality over this region.

Line 509-510: I get lost here. It is not clear to me that 58% contribution from China emissions is for outflow or something else. Authors need to clarify this.

Response:

Clarified as "The yearly contribution from emissions from China to outflow from East Asia in this study is 58%, similar to the contribution of 61% in Matsui et al. (2013) calculated based on eastward BC mass flux using WRF-CMAQ model with INTEX-B missions."

Line 531-538: I think the authors should list a table to compare your results with other studies, including annual BC emission budgets, burden, lifetime, DRF and DRF efficiency.

Response:

Thanks the suggestion. We have added Table S5 to compare these values with previous studies.

We have also added a discussion of this comparison in the manuscript, as "The total DRF of BC averaged over continental China simulated in this study is 2.27 W m^{-2}, larger than 0.64–1.55 W m^{-2} in previous studies (Wu et al., 2008; Zhuang et al., 2011; Li et al., 2016), probably due to the different emissions in the time periods of study, as shown in Table S5." And "The annual mean and regional mean DRF efficiency in China is 0.91 W m^{-2} Tg^{-1}, within the range of 0.41–1.55 W m^{-2} Tg^{-1} from the previous studies (Table S5)."

Table S5. Comparison of the simulated annual mean emission, burden, DRF and DRF efficiency in China in this study with the values reported in three previous studies.

Reference	Model	Year	Emission in China (Gg yr^{-1})	Burden (mg m^{-2})	DRF (Wm^{-2})	DRF efficiency (W m^{-2} Tg^{-1})
Wu et al. (2008)	RegCM3	2000	1005	0.55–1.42	0.64–1.55	0.64–1.55
Zhuang et al. (2011)	RegCCMS	2006	1811	1.12	0.75	0.41
Li et al. (2016)	GEOS-Chem	2010	1840		1.22	0.66
This study	CESM	2010–2014	2497	1.45	2.27	0.91

Line 654-655: Other modeling studies also found model low bias over China using CAWNET, e.g. Huang et al., 2013; Wang et al., 2014, which can be referenced here.
Huang, Y., S. Wu, M. K. Dubey, and N. H. F. French, Impact of aging mechanism on model simulated carbonaceous aerosols, Atmos. Chem. Phys., 13, 6329–6343, doi:10.5194/acp-13- 6329-2013, 2013.
Wang, Q., D.J. Jacob, J.R Spackman, A.E. Perring, J.P. Schwarz, N. Moteki, E.A. Marais, C. Ge, J. Wang and S.R.H. Barrett, Global budget and radiative forcing of black carbon aerosol: constraints from pole-to-pole (HIPPO) observations across the Pacific, J. Geophys. Res., 119, 195- 206, 2014.
Response:
Added.

Line 669: “and” is missing between “modeled” and “observed”.
Response:
Added.

References:

Zhang, L. M., Gong S. L., Padro J. and Barrie L.: A size-segregated particle dry deposition scheme for an atmospheric aerosol module, Atmos. Environ., 35, 549-560, doi:10.1016/S1352-2310(00)00326-5 ,2001.

Abdul-Razzak, H., and Ghan S. J.: A parameterization of aerosol activation: 2. Multiple aerosol types, J. Geophys. Res., 105, 6837–6844, doi:10.1029/1999JD901161, 2000.

Wang, H., R. C. Easter, P. J. Rasch, M. Wang, X. Liu, S. J. Ghan, Y. Qian, J.-H. Yoon, P.-L. Ma, and V. Vinoj (2013), Sensitivity of remote aerosol distributions to representation of cloud-aerosol interactions in a global climate model, Geosci. Model Dev., 6, 765–782, doi:10.5194/gmd-6-765-2013.

Hadley, O. L., V. Ramanathan, G. R. Carmichael, Y. Tang, C. E. Corrigan, G. C. Roberts, and G. S. Mauger (2007), Trans-Pacific transport of black carbon and fine aerosols (D < 2.5 μm) into North America, J. Geophys. Res., 112, D05309, doi:10.1029/2006JD007632.

Matsui, H., M. Koike, Y. Kondo, N. Oshima, N. Moteki, Y. Kanaya, A. Takami, and M. Irwin (2013), Seasonal variations of Asian black carbon outflow to the Pacific: Contribution from anthropogenic sources in China and biomass burning sources in Siberia and Southeast Asia, J. Geophys. Res. Atmos., 118, 9948–9967, doi:10.1002/jgrd.50702.

Yang Y., H. Liao, and S. Lou (2015), Decadal trend and interannual variation of outflow of aerosols from East Asia: Roles of variations in meteorological parameters and emissions, Atmos. Environ., 100, 141-153, doi:10.1016/j.atmosenv.2014.11.004.

Oshima, N., Y. Kondo, Moteki N., Takegawa N., Koike M., Kita K., Matsui H., Kajino M., Nakamura H., Jung J. S., and Kim Y. J.: Wet removal of black carbon in Asian outflow: Aerosol Radiative Forcing in East Asia (A-FORCE) aircraft campaign, J. Geophys. Res., 117, D03204, doi:10.1029/2011JD016552, 2012.

Huang, Y., S. Wu, M. K. Dubey, and N. H. F. French, Impact of aging mechanism on model simulated carbonaceous aerosols, Atmos. Chem. Phys., 13, 6329–6343, doi:10.5194/acp-13- 6329-2013, 2013.

Wang, Q., D.J. Jacob, J.R Spackman, A.E. Perring, J.P. Schwarz, N. Moteki, E.A. Marais, C. Ge, J. Wang and S.R.H. Barrett, Global budget and radiative forcing of black carbon aerosol: constraints from pole-to-pole (HIPPO) observations across the Pacific, J. Geophys. Res., 119, 195- 206, 2014.

Manuscript # acp-2016-1032

Responses to Reviewer #3

This study quantified source contributions of black carbon (BC) mass concentrations, trans-Pacific transport of BC, and direct radiative forcing of BC from seven regions in China using the Community Earth System Model with a source-tagging technique. The authors showed that BC concentrations were dominated by local emissions for regions with high emissions (e.g., North China, South China), whereas non-local emissions were important for regions with low emissions (e.g., Northwest China, Tibetan Plateau). They also showed that emissions from China and other regions were equally important for the BC outflow from East Asia and that emissions from China would be important for air quality in western United States. The annual mean direct radiative forcing of BC in China in their simulations was 2.3 W m^{-2}, and the contribution from emissions in China was estimated to be 66%.

The purpose of this study is interesting and the results obtained in this study are important to understand BC behavior in the atmosphere over East Asia. I think the authors should describe several points (shown below) more clearly, but overall the manuscript is written well and is suitable for the publication of this journal.

Major comments:

(1) Importance of BC in air quality problems
The authors sometimes use BC as an indicator of pollution (or air quality) in China (Lines 39-40, Lines 101-102, Lines 429-431, and Lines 571-572). However, I think it is questionable whether the concentrations and/or source contributions of BC can be used to represent those of total aerosols. Inorganic and organic species are dominant in China during polluted days, and spatial/temporal variations and source contributions of these species are largely different from those of BC because spatial distributions of emissions (e.g., BC v.s. SO2) and formation processes (primary v.s. secondary) are considerably different. For example, Matsui et al. (2009) showed that primary aerosols around Beijing were controlled by emissions within 100 km around Beijing within the preceding 24 h, while emissions as far as 500 km and within the preceding 3 days were found to affect secondary aerosols. Therefore, it is not always correct to extend the results of BC (e.g., source contributions) to the discussions on pollution and air quality because inorganic and organic species could have larger contributions from non-local emissions than BC. Please consider this point and describe the limitation of using BC results only in the discussions of air quality problems. In addition, please show the percentage of BC mass to total mass (PM2.5) in China in the manuscript.
Response:

Thanks for the suggestion. We have added a paragraph in the discussion section to describe the limitation of using BC results, as “In this study, BC is used as an indicator of pollution (or air quality) in China. It should be noted that, contributions of BC from different source regions may not fully represent source-receptor relationship of total aerosols. The contribution of BC to total near-surface PM2.5 (sum of BC, sulfate, primary organic matter and second organic carbon) concentration averaged over China is only about 10%. Inorganic and organic species aerosols, such as sulfate, are dominant in China during polluted days, and spatial/temporal variations and source contributions of these species are largely different from those of BC because spatial distributions of emissions (e.g., BC v.s. SO_2) and formation processes (primary v.s. secondary) are considerably different. For example, Matsui et al. (2009) showed that primary aerosols around Beijing were controlled by emissions within 100 km around Beijing within the preceding 24 h, while emissions as far as 500 km and within the preceding 3 days were found to affect secondary aerosols. Thus, the inorganic and organic species could have larger contributions from non-local emissions than BC. BC concentrations are highest in winter over China due to higher emissions, while sulfate concentrations reach maximum in summer because of stronger sunlight and higher temperature preferring sulfate formation. Therefore, knowing the accurate source attribution of air pollution in China requires source tagging for more aerosol species, such as sulfate.”

(2) Treatment of optical property and CCN activity of BC (Lines 151-169)
I could not find the description on the treatment of optical property (well-mixed, core-shell, or others) and CCN activity (conversion from hydrophobic to hydrophilic BC) of BC in the MAM3 model. I assume that well-mixed optical treatment is used to calculate BC absorption and that all BC particles are treated as hydrophilic BC in MAM3. Please describe the treatment of optical property and CCN activity of BC in the manuscript, and add some description on the potential impact (uncertainty) of these treatments on the estimation of BC concentrations, trans-Pacific transport of BC, AAOD, and direct radiative forcing of BC and their source contributions.
Response:
Thanks for the suggestion. We have added all these information in methods section and added a paragraph discussing the potential influence in conclusions and discussions section shown as below:
Aerosol optical properties for each mode are internally-mixed and parameterized according to Ghan and Zaveri (2007). Refractive indices for aerosols are taken from OPAC (Koepke and Schult, 1998), but for solar wavelengths of BC the value is from Bond and Bergstrom (2006). In MAM3, the aging process of BC is neglected by assuming the immediate mixing of BC with other aerosol species.
BC aging in the atmosphere is important for BC concentration and its optical properties, which transforms BC from hydrophobic aggregates to hydrophilic particles coated with soluble materials. He et al. (2015, 2016a) found BC optical properties varied by up to more than a factor of two due to different coating structures and aging stages during BC aging process based on theoretical and experimental

intercomparison. Oshima et al. (2009) and He et al. (2016b) pointed out that applying microphysical BC aging schemes could significantly improve simulations of BC concentrations compared with simplified aging parameterizations. Liu et al. (2012) also reported that the wet removal rate of BC simulated in standard CAM5 is 60% higher than AeroCom multi-model mean due to rapid or instantaneous aging of BC. H. Wang et al. (2013) showed that the explicit treatment of BC aging process with slower aging assumptions in CAM5 could significantly increase BC lifetime and the efficiency of BC long-range transport. In MAM3 aerosol module of CAM5 used in this study, the aging process of BC is neglected by assuming the immediate mixing of BC with other aerosol species. This assumption could lead to too much wet removal of BC and therefore underestimation of BC concentration, absorption optical depth (Fig. 3) and direct radiative forcing. In addition, the well-mixed optical treatment in CAM5 could also cause bias in BC absorption calculation. H. Wang et al. (2014) examined source-receptor relationships for BC and found that, with BC slow-aging treatment included in CAM5, the source region contributions to global BC burden only perturbed slightly compared to simulation without BC aging. Therefore, although the magnitude of simulated BC and its optical properties could be underestimated due to instantaneous aging of BC and uncertainty in coating structures, we expect the aging treatment in MAM3 of CAM5 may not influence the source contributions examined in this study. However, if the BC source-tagging technique could be implemented in future models with explicit BC aging processes, e.g. the new four-mode version (MAM4, Liu et al., 2016) of CAM version 5.3, with explicit optical property treatment, a more accurate source-receptor relationships of BC in China could be presented.

Other comments:

(3) Line 70
Please describe the reason of the faster regional removal.
Response:
Revised as “BC in East Asia has a shorter lifetime than the global mean value due to a faster regional removal (H. Wang et al., 2014), probably associated with strong precipitation during monsoon season.”

(4) Lines 168-169
Please clarify the definition of the direct radiative forcing of BC. Is this calculated from the difference of two radiative transfer calculations with and without BC for the clear-sky condition?
Response:
Revised as “Direct radiative forcing of BC is calculated from the difference of two radiative transfer calculations with and without BC for the all-sky condition following (Ghan, 2013).”

(5) Lines 182-204

Please show the difference of BC emission fluxes between the emission inventory used in this study and other emission inventories (e.g., INTEX-B, HTAP). The values are shown later (at Lines 534-538), but I think it is better to show them here. In addition, please add some comments on the impact of larger values of BC emissions in this study on the estimation of source contributions of BC. Can you add the values of BC emissions from outside China (e.g., India, Southeast Asia, Japan, Korea) to Figure 1b?

Response:

Thanks for the suggestion. We have added Table S1 to compare the anthropogenic emission used in this study with emissions from previous studies. The anthropogenic emission of BC in China for 2010–2014 is larger than those from previous studies, partly resulting from the rapid increasing trend of BC in China during recent years. The higher emission could lead to higher concentration and direct radiative forcing, and source contributions of BC in China. We have added these descriptions in methods section.

We also added BC emissions from outside China in Figure 1c. Emissions in continental level are summarized here instead of Country level because the model revolution is a bit course compared to country level emission. Total BC emissions from neighboring regions including, rest of East Asia (REA, without China), South Asia (SAS), Southeast Asia (SEA), and Russia/Belarussia/Ukraine (RBU) are shown in Figure 1c. The source regions outside China are consistent with regions source regions defined in the second phase of Hemispheric Transport of Air Pollution (HTAP2). South Asia and Southeast Asia have higher emissions, which may contribute to concentration and direct radiative forcing of BC in China, especially southern and western China, through long-range transport. We have also added these in the methods section.

Table S1. Comparisons of annual anthropogenic BC emissions in China with previous studies.

	Year	Anthropogenic emission in China (Gg/yr)
This study (CEDS, Hoesly et al., 2017)	2010–2014	2467
MIX (Li et al., 2017)	2010	1765
HTAP V2.2 (Janssens-Maenhout et al., 2015)	2010	1741
Lu et al. (2011)	2010	1751
Qin and Xie (2012)	2009	1764
Wang et al. (2012)	2007	1879
INTEX-B (Zhang et al., 2009)	2006	1811

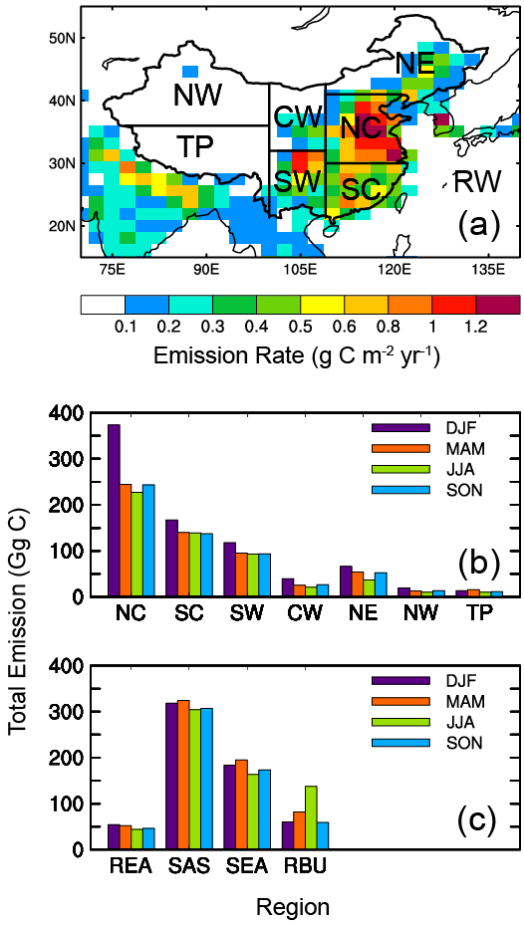

Figure 1. (a) Spatial distribution of annual mean total emissions (anthropogenic plus biomass burning, units: g C m^{-2} yr^{-1}) of black carbon (BC) averaged over 2010–2014. The geographical BC source regions are selected as North China (NC, 109°E–east boundary, 30°–41°N), South China (SC, 109°E–east boundary, south boundary–30°N), Southwest China (SW, 100°–109°N, south boundary–32°N), Central-West China (CW, 100°–109°N, 32°N–north boundary), Northeast China (NE, 109°E–east boundary, 41°N–north boundary), Northwest China (NW, west boundary–100°E, 36°N–north boundary), and Tibetan Plateau (TP, west boundary–100°E, south boundary–36°N) in China and regions outside of China (RW, rest of the world). (b) Seasonal mean total emissions (units: Gg C, Gg = 10^9g) of BC from the seven BC source regions in China and (c) emissions from rest of East Asia (REA without China), South Asia (SAS), Southeast Asia (SEA), and Russia/Belarussia/Ukraine (RBU).

(6) Lines 261-263

You can show the contributions from outside China quantitatively from the tagged simulation results.

Response:

We quantitatively showed the contributions from outside China in the results section. And it is not suitable to compare surface value and burden value. Therefore we have deleted this sentence to avoid duplicate and potential misleading.

(7) Line 281

Please describe the reason of BC underestimation by up to a factor of 20.

Response:

We have added a sentence, “where BC concentrations appear to be underestimated in the model (up to 20 times lower). The possible bias is discussed in the following part”, because we fully discussed this underestimation of BC in the following part and in the discussion section, as

“Note that the model largely underestimates BC concentrations over China, compared to the observation, which has also been reported in many previous studies using different models and different emission inventories (e.g., Liu et al., 2012; Fu et al., 2012; Huang et al., 2013; H. Wang et al., 2013; Q. Wang et al., 2014; R. Wang et al., 2014; Li et al., 2016). One possible reason is that in situ measurements are point observations, while the model does not treat the subgrid variability of aerosols and assumes aerosols are uniformly distributed over the grid cell. R. Wang et al. (2014) found a reduction of negative bias (from −88% to −35%) in the modeled surface BC concentrations when using high-resolution emissions and modeling at 0.5° X 0.7° resolution. They find, however, that modeling over the North China Plain at an even higher resolution of 0.1°, further reduced the surface concentration bias there from 29% to 8%. This result indicates that the siting of observational stations can result in an artificial bias when comparing with relatively coarse model results. Further investigation of this siting/resolution bias is warranted, including investigation if this

type of bias might extend, presumably to a lesser exent, also to AAOD measurements.

Further reasons that could contribute to this bias are emission underestimation or inaccurate aerosol processes in the model. Given that the differences between modeled and observed AAOD over eastern China are relatively small (–18%), we conclude that, given current evidence, the total amount of atmospheric BC in these simulations is reasonable at least in this sub-region.

Over eastern China, the BC concentrations are dominated by local emissions in this study, with local contribution of 64–93%. The underestimation of simulated BC concentrations over eastern China is more likely due to either underestimation of local emissions, too much aerosol removal within these regions, or resolution bias between observations and model grids. Over western China, 22–76% of the BC originates from emissions outside China. Thus biases of simulated BC concentrations could also come from underestimation of emissions outside China and or too much removal of BC during long-range transport. Satellite data are a promising method to validate modeling and emissions inventories, given that they do not depend on the location of observing stations, providing more uniform spatial coverage. A comparison of modeled AAOD and satellite aerosol index (AI) provides an indication that the modeled burden in western China is underestimated, although the role of dust needs to be better characterized."

(8) Line 343

I cannot find large sources of BC in Northwest China in Figure 1a. Does the description here mean that there may be large sources of BC which are not considered in the emission inventory? Can you show the contribution of BC and dust to AAOD (in model) over this region? I think dust is dominant over this region.

Response:

Yes. The uncertainty in emission over Northwest China could be one reason, as well as too much removal in local region. In the following source attribution analysis, we found emission from outside China also significantly contribute to BC concentration in Northwest China. Therefore the underestimation in BC concentration could also come from the uncertainty in emission outside China or too much removal during long-range transport in the model.

Correct, dust is dominant over Northwest China (Fig. A). The bias in dust simulation could also lead to the difference between model and observation. That is why we notice the potential bias from dust simulation, as "It is somewhat difficult to draw a firm conclusion, however, given the likely differential role of dust, and model biases modeling dust, and possible biases in satellite derived AI values." And "A comparison of modeled AAOD and satellite aerosol index (AI) provides an indication that the modeled burden in western China is underestimated, although the role of dust needs to be better characterized."

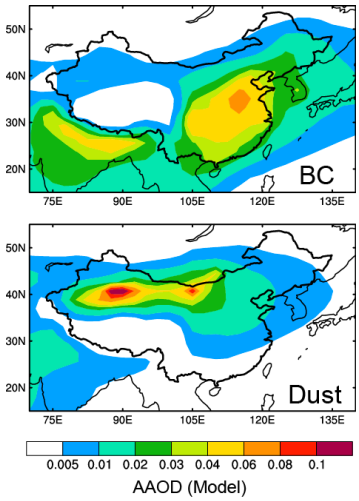

Figure A. Simulated annual mean AAOD of BC and dust.

(9) Lines 667-669

Related to the comment (2), is an internally-mixed treatment used in the calculations of AAOD? If so, AAOD should be lower (underestimated more) when more realistic BC mixing state treatment is used in the optical calculations.

Response:

Yes, CAM5 uses internally-mixed treatment in the calculations of AAOD. We have added a caveat here, as "Note that, the model uses internally-mixed treatment in the calculations of AAOD, indicating that the AAOD could be underestimated more in the model compared observations."

References:

Matsui, H., et al. (2009), Spatial and temporal variations of aerosols around Beijing in summer 2006: Model evaluation and source apportionment, J. Geophys. Res., 114, D00G13, doi:10.1029/2008JD010906.

Ghan, S. J., and R. A. Zaveri (2007), Parameterization of optical properties for hydrated internally mixed aerosol, J. Geophys. Res., 112, D10201, doi:10.1029/2006JD007927.

Bond, T. C., and R. W. Bergstrom, Light absorption by carbonaceous particles: An investigative review, Aerosol. Sci. Technol., 40, 27–67, doi:10.1080/02786820500421521, 2006.

872 Koepke, M. H. P., and I. Schult, Optical properties of aerosols and clouds: The
873 software package opac, Bull. Am. Meteorol. Soc., 79, 831–844, 1998,
874 doi:10.1175/1520-0477(1998)079<0831:OPOAAC>2.0.CO;2.
875
876 He, C., Liou, K.-N., Takano, Y., Zhang, R., Levy Zamora, M., Yang, P., Li, Q., and
877 Leung, L. R.: Variation of the radiative properties during black carbon aging:
878 theoretical and experimental intercomparison, Atmos. Chem. Phys., 15,
879 11967-11980, doi:10.5194/acp-15-11967-2015, 2015.
880
881 He, C., Takano, Y., Liou, K.-N., Yang, P., Li, Q., and Mackowski, D. W.:
882 Intercomparison of the GOS approach, superposition T- matrix method, and
883 laboratory measurements for black carbon optical properties during aging, J.
884 Quant. Spectrosc. Ra., 184, 287–296, doi:10.1016/j.jqsrt.2016.08.004, 2016a.
885
886 He, C., Li, Q., Liou, K.-N., Qi, L., Tao, S., and Schwarz, J. P.: Microphysics-based
887 black carbon aging in a global CTM: constraints from HIPPO observations and
888 implications for global black carbon budget, Atmos. Chem. Phys., 16, 3077-3098,
889 doi:10.5194/acp-16-3077-2016, 2016b.
890
891 Oshima, N., M. Koike, Y. Zhang, Y. Kondo, N. Moteki, N. Takegawa, and Y. Miyazaki
892 (2009), Aging of black carbon in outflow from anthropogenic sources using a
893 mixing state resolved model: Model development and evaluation, J. Geophys.
894 Res., 114, D06210, doi:10.1029/2008JD010680.
895
896 Liu, X., et al. (2012), Toward a minimal representation of aerosols in climate models:
897 Description and evaluation in the Community Atmosphere Model CAM5, Geosci.
898 Model Dev., 5, 709–739, doi:10.5194/gmd-5-709-2012.
899
900 Liu, X., Ma, P.-L., Wang, H., Tilmes, S., Singh, B., Easter, R. C., Ghan, S. J., and
901 Rasch, P. J.: Description and evaluation of a new four-mode version of the Modal
902 Aerosol Module (MAM4) within version 5.3 of the Community Atmosphere Model,
903 Geosci. Model Dev., 9, 505-522, doi:10.5194/gmd-9-505-2016, 2016.
904
905 Wang, H., R. C. Easter, P. J. Rasch, M. Wang, X. Liu, S. J. Ghan, Y. Qian, J.-H.
906 Yoon, P.-L. Ma, and V. Vinoj (2013), Sensitivity of remote aerosol distributions to
907 representation of cloud-aerosol interactions in a global climate model, Geosci.
908 Model Dev., 6, 765–782, doi:10.5194/gmd-6-765-2013.
909
910 Wang, H., P. J. Rasch, R. C. Easter, B. Singh, R. Zhang, P.-L. Ma, Y. Qian, S. J.
911 Ghan, and N. Beagley (2014), Using an explicit emission tagging method in
912 global modeling of source-receptor relationships for black carbon in the Arctic:
913 Variations, sources, and transport pathways, J. Geophys. Res. Atmos., 119,
914 12,888–12,909, doi:10.1002/ 2014JD022297.
915

916 Ghan, S. J. (2013), Technical Note: Estimating aerosol effects on cloud radiative
917 forcing, Atmos. Chem. Phys., 13, 9971-9974, doi:10.5194/acp-13-9971-2013.
918
919 Li, K., Liao, H., Mao, Y. H., and Ridley, D. A.: Source sector and region contributions
920 to concentration and direct radiative forcing of black carbon in China, Atmos.
921 Environ., 124, 351–366, doi:10.1016/j.atmosenv.2015.06.014, 2016.
922
923 Janssens-Maenhout, G., Crippa, M., Guizzardi, D., Dentener, F., Muntean, M.,
924 Pouliot, G., Keating, T., Zhang, Q., Kurokawa, J., Wankmüller, R., Denier van der
925 Gon, H., Kuenen, J. J. P., Klimont, Z., Frost, G., Darras, S., Koffi, B., and Li, M.:
926 HTAP_v2.2: a mosaic of regional and global emission grid maps for 2008 and
927 2010 to study hemispheric transport of air pollution, Atmos. Chem. Phys., 15,
928 11411-11432, doi:10.5194/acp-15-11411-2015, 2015.
929
930 Lu, Z., Zhang, Q., and Streets, D. G.: Sulfur dioxide and primary carbonaceous
931 aerosol emissions in China and India, 1996–2010, Atmos. Chem. Phys., 11,
932 9839-9864, doi:10.5194/acp-11-9839-2011, 2011.
933
934 Qin, Y. and Xie, S. D.: Spatial and temporal variation of anthropogenic black carbon
935 emissions in China for the period 1980–2009, Atmos. Chem. Phys., 12,
936 4825-4841, doi:10.5194/acp-12-4825-2012, 2012.
937
938 Wang, R., Tao, S., Wang, W., Liu, J., Shen, H., Shen, G., Wang, B., Liu, X., Li, W.,
939 Huang, Y., Zhang, Y., Lu, Y., Chen, H., Chen, Y., Wang, C., Zhu, D., Wang, X.,
940 Li, B., Liu, W., Ma, J.: Black carbon emissions in China from 1949 to 2050,
941 Environ. Sci. Technol., 46, 7595-7603, doi:10.1021/es3003684, 2012.
942
943 Zhang, Q., Streets, D. G., Carmichael, G. R., He, K. B., Huo, H., Kannari, A., Klimont,
944 Z., Park, I. S., Reddy, S., Fu, J. S., Chen, D., Duan, L., Lei, Y., Wang, L. T., and
945 Yao, Z. L.: Asian emissions in 2006 for the NASA INTEX-B mission, Atmos.
946 Chem. Phys., 9, 5131-5153, doi:10.5194/acp-9-5131-2009, 2009.
947

Source attribution of black carbon and its direct radiative forcing in China

Yang Yang[1], Hailong Wang[1*], Steven J. Smith[2], Po-Lun Ma[1], Philip J. Rasch[1]

[1]Atmospheric Science and Global Change Division, Pacific Northwest National Laboratory, Richland, Washington, USA

[2]Joint Global Change Research Institute, Pacific Northwest National Laboratory, College Park, Maryland, USA

*Correspondence to yang.yang@pnnl.gov and hailong.wang@pnnl.gov

Abstract

The source attributions for mass concentration, haze formation, transport, and direct radiative forcing of black carbon (BC) in various regions of China are quantified in this study using the Community Earth System Model (CESM) with a source-tagging technique. Anthropogenic emissions are from the Community Emissions Data System that is newly developed for the Coupled Model Intercomparison Project Phase 6 (CMIP6). Over North China where the air quality is often poor, about 90% of near-surface BC concentration is contributed by local emissions. 30% of BC concentration over South China in winter can be attributed to emissions from North China and 10% comes from sources outside China in spring. For other regions in China, BC is largely contributed from non-local sources. We further investigated potential factors that contribute to the poor air quality in China. During polluted days, a net inflow of BC transported from non-local source regions associated with anomalous winds plays an important role in increasing local BC concentrations. BC-containing particles emitted from East Asia can also be transported across the Pacific. Our model results show that emissions from inside and outside China are equally important for the BC outflow from East Asia, while emissions from China account for 7% of BC concentration and 25% in column burden in western United States in spring. Radiative forcing estimated shows that 66% of the annual mean BC direct radiative forcing (2.3 W m^{-2}) in China results from local emissions, and the remaining 34% are contributed by emissions outside of China. Efficiency analysis shows that reduction in BC emissions over eastern China could benefit more on the regional air quality in China, especially in winter haze season.

1. Introduction

Black carbon (BC), as a component of atmospheric fine particulate matter ($PM_{2.5}$), is harmful to human health (Anenberg et al., 2011; Janssen et al., 2012). In addition to its impact on air quality, as the most efficient light-absorbing anthropogenic aerosols, BC is thought to exert a substantial influence on climate (Bond et al., 2013; IPCC, 2013; Liao et al., 2015). It can heat the atmosphere through absorbing solar radiation (Ramanathan and Carmichael, 2008), influence cloud microphysical and dynamical processes (Jacobson, 2006; McFarquhar and Wang, 2006), and reduce surface albedo through deposition on snow and ice (Flanner et al., 2007; Qian et al., 2015).

Due to accelerated urbanization and rapid economic growth, emissions of BC in China increased dramatically during recent decades. It contributed to about one fourth of the global emissions of BC in recent decades (Bond et al., 2007). Strong emissions lead to high concentrations of BC over China. Zhang et al. (2008) collected aerosol samples at eighteen stations spread over China during 2006 and reported BC concentrations in a range of 9–14 μg m^{-3} at urban sites, 2–5 μg m^{-3} at rural sites, and about 0.35 μg m^{-3} at remote background sites. BC also exerts significant positive direct radiative forcing (DRF) at the top of the atmosphere (TOA) in China. Using the Regional Climate Chemistry Modeling System (RegCCMs), Zhuang et al. (2013) reported an annual mean BC DRF of 2–5 W m^{-2} at TOA over eastern China and about 6 W m^{-2} over Sichuan Basin in year 2006. Li et al. (2016) also showed a strong DRF of BC over the North China Plain and Sichuan Basin in most seasons except for spring when the strongest BC DRF with values of 4–6 W m^{-2} shifted to southern China.

BC is the product of incomplete combustion of fossil fuels, biofuels, and open burning, such as forest and grassland fires and agricultural waste burning on fields. In the atmosphere the average lifetime of BC is only a few days, due to both wet removal and dry deposition, which is much shorter than that of long-lived greenhouse gases. In addition, BC lifetime is region dependent. BC in East Asia has a shorter lifetime than the global mean value due to a faster regional removal (H. Wang et al.,

Yang Yang 1/31/2017 2:23 PM
Deleted: 18

2014), probably associated with strong precipitation during monsoon season. BC emission reductions may benefit both mitigation of global climate change and regional air quality (Shindell et al., 2012; Bond et al., 2013; Smith and Mizrahi, 2013), especially in East Asia where fuel combustion emits substantial BC along with other pollutant species. Many previous observational and/or modeling studies have examined the source sector contributions of BC over China (Zhuang et al., 2014; Y.-L. Zhang et al., 2015; Li et al., 2016). They found that residential heating and industry sectors were the largest contributors to BC concentrations in China, while biomass burning emissions from outside China were important to BC in western China. An effective BC reduction in a receptor region would require knowing not only the source sector that contributes the most to BC levels, but also the source contributions from various locations within and outside the region. However, very few previous studies have focused on the source attribution of BC concentrations in various regions of China. Li et al. (2016) examined the contributions of emissions inside and outside China to BC over China (with only two source regions) but did not divide the source contributions from different regions inside China.

Pollution levels also show substantial daily to weekly variation. In recent years, extreme wintertime hazy conditions occurred frequently in China and caused serious air pollution, affecting more than half of the 1.3 billion people (Ding and Liu, 2014). During one winter haze episode in 2013, BC concentrations increased up to about 20 and 8 μg m^{-3} in Xi'an and Beijing over northern China, and 6 and 4 μg m^{-3} in Guangzhou and Shanghai over southern China, respectively (Y.-L. Zhang et al., 2015). The transport of pollutants from upwind was reported to be one of the most important contributors to local high aerosol concentrations during haze days (L. T. Wang et al., 2014; Y. Yang et al., 2016). L. T. Wang et al. (2014) found that emissions from northern Hebei and Beijing-Tianjin were the major contributor to particulate matter ($PM_{2.5}$) pollution in Shijiazhuang in January 2013. Yang et al. (2016) confirmed a connection between wind fields and $PM_{2.5}$ concentrations during winter hazy days through model simulations and statistical analysis. They also found that weakened winds contributed to increases in winter aerosol concentrations and hazy days over

eastern China during recent decades. As a chemically inert species, atmospheric BC is a good tracer to investigate the source region contributions from local and non-local emissions during polluted conditions that are related to long-range transport.

BC particles originating from East Asia can also be transported across the North Pacific, reaching North America (Hadley et al., 2007; Ma et al., 2013a; Matsui et al., 2013; H. Wang et al., 2014; Yang et al., 2015). Matsui et al. (2013) simulated outflow of BC from East Asia using the Community Multiscale Air Quality (CMAQ) model and found that anthropogenic emissions from China, biomass burning emissions from Southeast Asia, and biomass burning emissions from Siberia and Kazakhstan contributed 61%, 17%, and 6%, respectively, to the eastward BC flux at 150°E averaged over 2008–2010. Hadley et al. (2007) estimated the trans-Pacific transport of BC during April of 2004 using the Chemical Weather Forecast System (CFORS) model and reported that, across 130°W, 75% of BC transported into North America originated from Asia. Huang et al. (2012) simulated BC using the Sulfur Transport and Deposition Model (STEM), and found emissions outside North America contributed to 30–80% of column BC over North America in summer 2008. H. Wang et al. (2014) examined the long-term (1995-2005) average global source-receptor relationship of BC and found that BC emitted from the entire East Asia only contribute less than 5% to the total BC burden in North America, although the contribution is up to 40% near the west coast region. Few studies have examined the outflow from East Asia and inflow into North America contributed from source regions in and outside China. In addition, the emissions of BC from China increased dramatically during the last few years, with the annual total anthropogenic emissions estimated to have almost doubled in year 2014 compared to year 2000, shown in the newly developed Community Emissions Data System (CEDS; Hoesly et al. 2017). Therefore, the long-range transport of BC and source-receptor relationships could be quite different from previous studies.

Due to its warming effect in the climate system, BC is potentially important for climate mitigation and has drawn much attention recently. Source attribution of the direct radiative effect of BC is likely to be different from that of near-surface

concentration and column burden due to the dependence of radiative forcing on the vertical distribution of BC and its mixing state with other species that are influenced by different regional sources. In this study, we use the Community Earth System Model (CESM) with improved representations of aerosol transport and wet removal (H. Wang et al., 2013) and a BC source-tagging technique (H. Wang et al., 2014). Anthropogenic emissions from the newly developed CEDS inventory (Hoesly et al., 2017), as released for the Coupled Model Intercomparison Project Phase 6 (CMIP6), are used to examine the source attributions for mass concentration, long-range transport, and direct radiative forcing of BC in various regions of China. We aim to quantify: (1) source region contributions to concentrations of BC over various receptor regions in China; (2) contributions to changes in BC concentrations under polluted conditions; (3) source contributions to trans-boundary and trans-Pacific transport of BC; and (4) source contributions to direct radiative forcing of BC in China.

The CESM model, emissions, and numerical experiment are described in Section 2. Section 3 provides evaluation of the simulated concentration and aerosol absorption optical depth of BC in China. Section 4 investigates source contributions to near-surface concentrations, long-range transport and direct radiative forcing of BC over various receptor regions using the BC source-tagging technique in CESM. Section 5 summarizes these results.

2. Methods

We simulate the evolution and direct radiative forcing (DRF) of BC using CESM version 1.2 (Hurrell et al., 2013). The atmospheric model in CESM is version 5 of the Community Atmosphere Model (CAM5), with horizontal grid spacing of 1.9° latitude by 2.5° longitude and 30 vertical layers ranging from the surface to 3.6 hPa used in this study. The model treats the properties and processes of major aerosol species (sea salt, mineral dust, sulfate, black carbon, primary organic matter and secondary organic aerosol) using a three-mode modal aerosol module (MAM3), in which aerosol size distributions are represented by three lognormal modes: Aitken, accumulation, and coarse modes. BC is emitted to the accumulation mode. Mass mixing ratios of

different aerosol species and the number mixing ratio are predicted for each mode. A more detailed description of the MAM3 representation can be found in Liu et al. (2012). Aerosol dry deposition velocities are calculated using the Zhang et al. (2001) parameterization. The wet deposition of aerosols in our CAM5 model includes in-cloud wet removal (i.e., activation of interstitial aerosols to cloud-borne particles followed by precipitation scavenging) and below-cloud wet removal (i.e., capture of interstitial aerosol particles by falling precipitation particles) for both stratiform and convective clouds. Aerosol activation is calculated with the parameterization of Abdul-Razzak and Ghan (2000) for stratiform cloud throughout the column and convective cloud at cloud base, while the secondary activation above convective cloud base has a simpler treatment with an assumed maximum supersaturation in convective updrafts (H. Wang et al., 2013). The unified treatment for convective transport and aerosol wet removal along with the explicit aerosol activation above convective cloud base was developed by H. Wang et al. (2013) and included in the CAM5 version being used in this study. This implementation reduces the excessive BC aloft and better simulates observed BC concentrations in the mid- to upper-troposphere. Aerosol optical properties for each mode are parameterized according to Ghan and Zaveri (2007). Refractive indices for aerosols are taken from the OPAC (optical properties for aerosols and clouds) software package (Koepke and Schult, 1998), but for BC at solar wavelengths the values are updated from Bond and Bergstrom (2006). In MAM3, the aging process of BC is neglected by assuming the immediate mixing of BC with other aerosol species. Direct radiative forcing of BC is calculated as the difference in the top-of-the-atmosphere net radiative fluxes with and without BC for the all-sky condition following Ghan (2013).

Anthropogenic emissions used in this study are from the CEDS dataset, as released for the CMIP6 model experiments (Hoesly et al. 2017). This newly released emission inventory includes aerosol (black carbon, organic carbon) and aerosol precursor and reactive compounds (sulfur dioxide, nitrogen oxides, ammonia, carbon monoxide, and non-methane volatile organic compounds). The emissions are provided at monthly resolution for each year of 1750–2014 on a 0.5° x 0.5° grid and

include agricultural, energy, industry, residential, international shipping, solvents, surface transportation, waste treatment, and aircraft sectors. The biomass burning emissions used in this study are also developed for CMIP6 based on Global Fire Emission Database (GFED) version 4, Fire Model Intercomparison Project (FireMIP), visibility-observations and Global Charcoal Database (GCD) data (van Marle et al. 2016).

Figure 1a shows the horizontal spatial distribution of annual emissions of BC averaged over the most recent 5 years (2010–2014) and the seven geographical source regions tagged in continental China, including North China (NC), South China (SC), Southwest China (SW), Central-West China (CW), Northeast China (NE), Northwest China (NW), and Tibetan Plateau (TP). Figure 1b summarizes the total seasonal BC emissions in each of these source regions. North China has the largest annual emissions of BC in China, with maximum emission larger than 1.2 g C m^{-2} $year^{-1}$ and a regional total emission of 1089 Gg C $year^{-1}$ (44% of total emissions from continental China). Annual emissions of BC also have large values over South and Southwest China, with maximum values in the range of 0.8–1.2 g C m^{-2} $year^{-1}$, followed by Central-West and Northeast China. Over the less economically developed Northwest China and remote region Tibetan Plateau, emissions of BC are much lower than other regions in China. The seasonal mean emissions of BC also show the same spatial pattern as the annual means. BC had the largest emissions over North, South, and Southwest China in all seasons, among which emissions are strongest in December-January-February (DJF), especially over North China, resulting from domestic heating. The total seasonal emissions of BC in continental China are 797, 586, 537, and 577 Gg C in DJF, March-April-May (MAM), June-July-August (JJA), and September-October-November (SON), respectively, which add up to a total annual BC emissions of 2497 Gg C averaged over years 2010–2014. The anthropogenic emissions of BC in China in 2010–2014 are larger than those used in the previous studies for earlier years (Table S1), partly as a result of a higher estimate of BC emissions from coal coking production. The higher emissions likely lead to higher concentrations and direct radiative forcing, and source

Yang Yang 1/31/2017 2:46 PM
Deleted: China

Yang Yang 1/31/2017 2:46 PM
Deleted: China

Yang Yang 1/31/2017 2:46 PM
Deleted: China

Yang Yang 1/31/2017 2:46 PM
Deleted: China

contributions of BC in China, compared to the values reported in these studies. The DJF emissions account for 26–35% of annual total whereas emissions in JJA only account for 17–24% over the seven source regions in continental China. Total BC emissions from neighboring regions including rest of East Asia (REA, with China excluded), South Asia (SAS), Southeast Asia (SEA), and Russia/Belarussia/Ukraine (RBU) are shown in Figure 1c. These source regions outside China are consistent with source regions defined in the second phase of Hemispheric Transport of Air Pollution (HTAP2). South Asia and Southeast Asia have relatively high emissions. They may dominate the contribution to concentrations and direct radiative forcing of BC in China, especially southern and western China, from foreign sources through long-range transport.

An explicit BC source tagging capability was originally implemented in CAM5 by H. Wang et al. (2014), through which emissions of BC from independent source regions and/or sectors can be explicitly tracked. This method quantifies the source–receptor relationships of BC in any receptor region within a single model simulation without perturbing emissions from individual source regions or sectors. R. Zhang et al. (2015a,b) used this method to quantify the source attributions of BC in western North America, Himalayas, and Tibetan Plateau. The same BC source tagging technique is implemented to a newer model version (CAM5.3) and applied in this study to quantify the source attributions of concentration, transport and direct radiative forcing of BC in various regions of China. BC emissions (anthropogenic plus biomass burning) from seven geographical source regions, including North China, South China, Southwest China, Central-West China, Northeast China, Northwest China, Tibetan Plateau in China, and from rest of the world (RW) are tagged. Transport and physics tendencies are calculated separately for each tagged BC in the same way as the original BC simulation in CESM. We choose the seven individual regions (North China, South China, Southwest China, Central-West China, Northeast China, Northwest China, and Tibetan Plateau) and all seven regions combined (hereafter continental China) as receptor regions in this study to examine the source-receptor relationships of BC. While all emissions, including sulfur dioxides,

organic carbon and BC, were used in the model simulation, tagging was only applied to BC emissions.

The CAM5 simulation is performed at 1.9° × 2.5° horizontal grid spacing using the specified-dynamics mode (Ma et al., 2013b), in which large-scale circulations (i.e., horizontal winds) are nudged to 6-hourly reanalysis data from the Modern Era Retrospective-Analysis for Research and Applications (MERRA) reanalysis data set (Rienecker et al., 2011) with a relaxation time scale of 6 hours (K. Zhang et al., 2014). The use of nudged winds allows for a more accurate simulation so that the key role of large-scale circulation patterns matches observations over the specified years. The simulation is run from year 2009 to 2014, with both time-varying aerosol emissions and meteorological fields. The first year is for spin-up and the last five years are used for analysis.

3. Model evaluation

The simulations of aerosols, especially BC, using CAM5 have been extensively evaluated against observations including aerosol mass and number concentrations, vertical profiles, aerosol optical properties, aerosol deposition, and cloud-nucleating properties in several previous studies (e.g., Liu et al., 2012, 2016; H. Wang et al., 2013; Ma et al., 2013b; Jiao et al., 2014; Qian et al., 2014; R. Zhang et al., 2015a,b). Here we focus on the evaluation of model performance in China using measurements of near-surface BC concentrations, vertical profiles, aerosol index derived from satellite, and aerosol absorption optical depth from the Aerosol Robotic Network (AERONET).

3.1 Mass concentrations and column burden of BC

Figure 2 presents spatial distributions of simulated seasonal mean near-surface concentrations and column burden of BC, both of which show a similar spatial pattern to emissions of BC (Figure 1a) with the largest values over North China and the lowest values over Northwest China and Tibetan Plateau. Near-surface model results are taken to be the lowest model layer (from surface to 985 hPa in average). Among all seasons, DJF has the highest BC levels, with values in the range of 6–12, 2–8,

Yang Yang 1/26/2017 2:39 PM
Deleted: many

Yang Yang 1/17/2017 2:34 PM
Deleted: Near-surface m

Yang Yang 1/31/2017 3:04 PM
Deleted: 993

and 1–8 μg m^{-3} for near-surface concentrations and 5–9, 3–7, 2–9 mg m^{-2} for column burden over North, South, and Southwest China, respectively. In contrast, JJA has the lowest BC concentrations over China due to the lower emissions and larger wet scavenging associated with East Asian summer monsoon (Lou et al., 2016). Averaged over continental China, near-surface BC concentrations are 2.2, 1.1, 0.8, and 1.3 μg m^{-3} in DJF, MAM, JJA, and SON, respectively, with seasonal variability of 38%. The column burden of BC shows smaller seasonal variability (26%), with area-weighted average of 1.9, 1.4, 1.1, and 1.3 mg m^{-2} in DJF, MAM, JJA, and SON, respectively, in China. The magnitude, spatial distribution, and seasonal variations of simulated near-surface BC concentrations over China are similar to those in Fu et al. (2012) and X. Wang et al. (2013) using Intercontinental Chemical Transport Experiment-Phase B (INTEX-B) emission inventory (Zhang et al., 2009) and those in Li et al. (2016) using HTAP emission inventory (Janssens-Maenhout et al., 2015) together with a global chemical transport model.

The simulated near-surface BC concentrations are evaluated here using measurements at fourteen sites of the China Meteorological Administration Atmosphere Watch Network (CAWNET) (Zhang et al., 2012). The locations of CAWNET sites are shown in Figure S1a. The observational data include monthly BC concentrations in years 2006–2007. Note that the simulated BC concentrations are for years 2010–2014. Figure 3a compares the simulated seasonal mean near-surface BC concentrations with those from CAWNET observations and Table S2 summarizes the comparison in different regions, using modeled values from the grid cell containing each observational site. Simulated BC concentrations at most sites are within the range of one third to three times of observed values, except for Dunhuang (94.68°E, 40.15°N) and Lhasa (91.13°E, 29.67°N) sites over western China, where BC concentrations appear to be underestimated in the model (up to 20 times lower). The possible bias is discussed in the following part. Over North China, simulated concentrations are similar to observations in DJF, but underestimated in other seasons. Over South China, the simulations do not have large biases compared to the observed BC. However, simulated BC is underestimated in all seasons over

Yang Yang 1/19/2017 3:23 PM
Deleted: It suggests that, besides domestic emissions in China, there are other BC sources from outside China contributing significantly to BC concentrations in the column.

Yang Yang 1/20/2017 6:17 PM
Deleted: Hemispheric Transport of Air Pollution (

Yang Yang 1/20/2017 6:17 PM
Deleted:)

Yang Yang 1/31/2017 3:07 PM
Deleted: 14

Yang Yang 1/31/2017 3:08 PM
Deleted: 3

Southwest, Central-West, Northeast, Northwest China, and Tibetan Plateau. Compared to the CAWNET data, the modeled near-surface BC concentrations have a normalized mean bias (NMB) of –53%. Note that anthropogenic BC emissions went up by a factor of 1.18 between 2006–2007 and 2010–2014. An emissions adjusted comparison would result in an even larger underestimation. There are several reasons that might cause low bias in this comparison. Liu et al. (2012) and H. Wang et al. (2013) have previously found underestimation of BC concentrations over China in CAM5 model and suggested the BC emissions may be significantly underestimated. Using the global chemical transport model GEOS-Chem together with emissions in 2006, Fu et al. (2012) found the simulated BC concentrations in China were underestimated by 56%. With HTAP emissions at the year 2010 level, Li et al. (2016) showed a low bias of 37% in simulated BC concentration in China. Larger wet removal rate and shorter lifetime of aerosols along with the instantaneous aging of BC in the MAM3 can also lead to the lower concentrations of BC (e.g., Wang et al., 2011; Liu et al., 2012; H. Wang et al., 2013; Kristiansen et al., 2016).

Another potential cause for a bias in this comparison is spatial sampling bias. Half of the CAWNET sites are located in urban areas, which will tend to have high values near sources, whereas the modeled values represent averages over large grid cells (R. Wang et al., 2014), as further discussed below.

The model captures well the spatial distribution and seasonal variation of BC concentrations in China, having a statistically significant correlation coefficient of +0.58 between simulated and observed seasonal BC concentrations over CAWNET sites.

Yang Yang 1/31/2017 3:14 PM
Deleted: between modeled and

Yang Yang 1/31/2017 3:14 PM
Deleted: values

Figure S2 compares the observed and simulated vertical profiles of BC concentrations in the East-Asian outflow region. The model successfully reproduces the vertical profile of BC that was measured in March–April 2009 during the A-FORCE field campaign and reported by Oshima et al. (2012).

3.2 Aerosol absorption optical depth of BC

To evaluate the simulated aerosol absorption optical depth (AAOD) of BC, the AAOD data from AERONET (Holben et al., 2001) are used here. The locations of

AERONET sites in China are shown in Figure S1b. The observed AAOD are averaged over years of 2010–2014 over seven sites and 2005–2010 over three sites with data available. Most AERONET sites are over eastern and central China. AAOD of BC at 550nm are calculated by interpolating AAOD at 440 and 675 nm and removing AAOD of dust from the retrieved AERONET AAOD following Bond et al. (2013). Figure 3b compares the observed and simulated seasonal mean AAOD of BC at 550nm and Table S3 summarizes the comparisons in different regions. The model has a low bias in simulating AAOD of BC in China, smaller than the bias in near-surface concentrations, with a NMB of –16%. As is the case with surface concentrations, this bias could be due to model issues, such as BC transport or optical parameterization; an underestimate in emissions; or spatial sampling bias. Simulated AAOD of BC are within the range of one third to three times of observed values at most sites, with the spatial distribution and seasonal variation broadly captured by the model. All but one of the observations are located in the North and South China regions, and simulated BC AAOD are, on average, similar to observations there. The AAOD from one observation site in Central-West China is higher than the modeled value. Note that, the observed AAOD of BC is derived from AERONET measurements using the absorption Ångström exponent. A recent study (Schuster et al., 2016) reported that absorption Ångström exponent is not a robust parameter for separating out carbonaceous absorption in the AERONET database, which could cause biases in the AAOD estimates.

Figure 4 shows the spatial distribution of simulated seasonal mean AAOD of total aerosols and Aerosol Index (AI) derived from Ozone Monitoring Instrument (OMI) measurements over years of 2010–2014. AI is a measure of absorbing aerosols including BC and dust. Compared to satellite AI data, the model roughly reproduces spatial distribution of total AAOD in China, with large values over North, South, and Southwest China in all seasons. AI derived from Total Ozone Mapping Spectrometer (TOMS) measurements (Figure S3) also shows similar pattern as simulated AAOD. It should be noted that, besides BC, dust particles also largely contribute to AI and produces large AI values over Northwest China.

Yang Yang 1/31/2017 3:23 PM
Deleted: 7

Yang Yang 1/31/2017 3:23 PM
Deleted: 3

Yang Yang 1/31/2017 3:24 PM
Deleted: (Figure 3a)

Yang Yang 1/31/2017 3:26 PM
Deleted: , although spatial sampling bias is likely to be less important for the BC column than for surface concentrations

Yang Yang 1/31/2017 3:26 PM
Deleted: 3

Yang Yang 1/31/2017 3:27 PM
Deleted: Note that a

Hailong Wang 2/1/2017 12:09 PM
Deleted: some

Yang Yang 1/18/2017 11:11 AM
Deleted: from

Yang Yang 1/18/2017 11:11 AM
Deleted: spatial

Yang Yang 1/31/2017 3:29 PM
Deleted: (Figure S3)

To examine the potential model bias more broadly we compared the difference of AAOD and AI between western and eastern China (Fig. 4). Averaging AI and AAOD broadly over eastern and western China, we find that AAOD/AI is 0.048 over eastern China and 0.031 over western China. If we assume that the simulated AAOD do not have large biases over eastern China based on the evaluation against observations shown above (Fig. 3b and Table S3), then this difference hints a possible underestimation of BC column burden in the model over the western regions. However, it is difficult to draw a firm conclusion, given the likely differential role of dust in eastern vs western China. This differential likely also contributes to AAOD biases in modeling dust and may also impact biases in the satellite derived AI values.

Yang Yang 1/31/2017 3:30 PM
Deleted: China

Yang Yang 1/27/2017 10:29 AM
Deleted: If we assume the simulated AAOD do not have large bias over eastern China compared to observations, then this difference hints at a possible underestimation of BC column burden in the model over the western regions. It is somewhat difficult to draw a firm conclusion, however, given the likely differential role of dust, and model biases modeling dust, and possible biases in satellite derived AI values.

Yang Yang 2/1/2017 1:32 PM
Formatted: Indent: First line: 0"

4. Source contributions to BC concentrations, transport and direct radiative forcing

4.1. Source contributions to seasonal mean BC concentrations

Figure 5 shows the simulated spatial distribution of seasonal near-surface BC concentrations originating from the seven tagged source regions in continental China and all other sources from outside China (rest of the world, RW) and Table S4 summarizes these source-receptor relationships. It is not surprising that regional emissions largely influence BC concentrations in the same region. For example, emissions of BC from North China give 5.8 μg m^{-3} of BC concentrations over North China in DJF, whereas they only account for less than 1.3 μg m^{-3} over other regions in China. However, the relatively small amount of BC from upwind source regions can also be a large contributor to receptor regions near the strong sources. BC emissions from North China contribute large amount to concentrations over South, Southwest, Central-West, and Northeast China. BC emissions from South and Southwest China also produce a widespread impact on BC over other neighboring regions. The impacts of BC emitted from the remaining China regions are relatively small both in local and non-local regions due to weak emissions (Fig. 1b). All the sources in China have the largest impact in DJF, resulting from the strong BC emissions in winter, while emissions from outside China have the largest impact on BC over China in

MAM due to the seasonal high emission over Southeast Asia and the strong springtime southwesterly winds.

Yang Yang 1/31/2017 3:35 PM
Deleted: biomass burning

Averaged over continental China, emissions of BC from North China produce mean BC concentrations of 0.4–1.1 μg m^{-3}, followed by 0.2–0.4 μg m^{-3} from South China and 0.1–0.2 μg m^{-3} from Southwest China emissions. For emissions over Central-West China, Northeast China, Northwest China, and Tibetan Plateau, their individual impact is less than 0.15 μg m^{-3}. In contrast, emissions from outside China result in 0.13 μg m^{-3} of BC concentrations in China in MAM and less than 0.10 μg m^{-3} in other seasons. The simulated source contributions to column burden of BC are shown in Figure S4. They present a very similar spatial distribution and seasonal variation to those of near-surface BC concentrations. However, the emissions from outside China have a larger impact on the average column burden of BC over China than on surface concentrations, with a magnitude of 0.5 mg m^{-2} in MAM, which is as the same as that from sources in North China.

Figure 6 shows the spatial distribution of simulated relative contributions to near-surface BC concentrations from sources in the seven regions in continental China and those outside China by season. (The same plots for BC column burden are shown in Figure S5.) For regions with higher emissions, their BC concentrations are dominated by local emissions. In contrast, BC levels, especially column burden of BC, over central and western China with lower emissions are strongly influenced by non-local sources. Emissions from outside China can be the largest contributor to BC over these regions. During DJF, MAM and SON, they contribute more than 70% to both surface concentrations and column burden of BC in Tibetan Plateau, which is important to the climate change due to the large climate efficacy of BC in snow (Qian et al., 2011) and acceleration of snowmelt through elevated BC heat pump mechanism (Lau et al., 2010). BC emissions from outside China also account for a quite significant fraction of surface concentrations over Northwest and Southwest China in MAM, which contribute to poor air quality over these regions.

Figure 7 summarizes source attribution for spatially averaged seasonal surface BC concentrations for the seven receptor regions and continental China combined

(CN). Over North China, the majority of the BC concentrations are attributed to local emissions in all seasons, with seasonal fractional contributions of 83–93%. Over South China, the seasonal contributions from local emissions are in the range of 64–87%. Emissions from North China account for 30% of BC concentrations over South China in DJF, resulting from the wintertime northwesterly winds (Figure S6a), while emissions from outside China contribute about 10% in MAM due to the strong springtime biomass burning over southeast Asia and southwesterly winds transporting BC from southeast Asia to South China (Figure S6b). Southwest China has a similar level of local influence, with 59–79% of the BC concentration from local emissions, whereas 17% are due to emissions from outside China transported by westerly winds in MAM.

Yang Yang 1/31/2017 4:11 PM
Deleted: world

Non-local emissions from Southwest and North China contribute 27–49% of BC concentration in Central-West China. North China emissions play an important role in BC concentrations over Northeast China, with relative contributions in a range of 22–36% in MAM, JJA and SON, while only 12% in DJF, which is associated with northwesterly winds in winter preventing northward transport of BC from North China to Northeast China. Over Northwest China and Tibetan Plateau, 22–40% and 43–76%, respectively, of BC originate from emissions outside China due to the low emissions over the less economically developed western China. For all of continental China as the receptor, the seasonal BC concentrations are largely attributed to the emissions from North and South China, with relative contributions ranging from 43–50% and 18–24%, respectively, followed by contributions from Southwest China (10–13%) and outside China (4–12%).

Yang Yang 1/31/2017 4:12 PM
Deleted: China

The source region contributions to column burden of BC in each receptor regions in China are shown in Figure S7. In general, impacts on the non-local BC column burden are larger than on surface concentrations because aerosol transport is relatively easier in free-troposphere than in the boundary layer (e.g., Yang et al., 2015). Column burdens of BC averaged over continental China mainly originate from emissions in North China, South China and outside China, with relative contributions ranging from 31–42%, 16–24% and 14–31%, respectively.

Yang Yang 1/27/2017 10:29 AM
Deleted: result

4.2. Source contributions during polluted days

Knowing the source attribution of BC during polluted days in China is important for policy makers, which could provide an effective way for the mitigation of poor air quality. Here, the polluted days are simply identified as days with daily concentrations of BC higher than 90th percentile of probability density function in each receptor regions. A total of different 45 days in winter in the 5-year simulation are identified as polluted days for each region in China.

Figure 8 shows the DJF composite differences in near-surface BC concentrations and winds at 850 hPa between polluted and normal days for each receptor region, and Figure 9 summarizes the local and non-local source contributions to the differences. When North China is under the polluted condition, BC concentrations are higher by more than 70% compared to DJF average over North China, with a maximum increase exceeding 5 μg m^{-3}. North China local emissions contribute 5.4 μg m^{-3} to the averaged increase in BC concentrations over North China during North China polluted days, about 90% of the total increase. In winter, eastern China is dominated by strong northwesterly winds (Figure S6a). The anomalous southerly winds during polluted days (relative to DJF average) over North China prevent the high BC concentrations from being transported to South China, leading to a reduced ventilation and accumulated aerosols in North China.

Over South China, BC concentrations increase by up to 2 μg m^{-3}, in part due to the transport from North China by anomalous northerly winds in the north part of South China in South China polluted days. On average, contribution of North China emissions to mean concentrations over South China increases by 1.2 μg m^{-3} (48% of total increase) during the South China polluted days.

During polluted days in Southwest China, the anomalous northeasterly winds in the east part of Southwest China bring in BC from the highly polluted eastern China, resulting in 1.1 μg m^{-3} increase (53% of total increase) in the Southwest China, which is as similar magnitude as the 1.0 μg m^{-3} contribution from the Southwest China local emissions.

Yang Yang 1/31/2017 4:16 PM
Deleted: (Fig. 2a)

Yang Yang 1/18/2017 11:35 AM
Deleted: S5a

The increase in BC concentrations during polluted days over Central-West China is also largely influenced by the accumulation effect of the anomalous winds over eastern and central China, which also transport BC from Southwest and eastern China into the receptor region.

The polluted days in Northeast China are caused by both the accumulation of local emissions due to the reduced prevailing northeasterly winds and anomalous transport of BC from North China.

Emissions from outside China could contribute to increases in BC concentrations over Northwest China and Tibetan Plateau during polluted days. However, during wintertime regional polluted days in eastern and central China, the contributions of emissions from outside China do not have a significant influence on the changes in BC concentrations.

These results suggest that the transport of aerosols plays an important role in increasing BC concentrations during regional polluted days in eastern and central China. Reductions in local emissions could benefit mitigation of both local and non-local haze in China. Emissions from outside China are not as important to hazy pollution in eastern and central China, where haze episodes occur frequently in winter due to relatively high anthropogenic aerosol emissions and abnormal meteorological conditions (Sun et al., 2014; R. H. Zhang et al., 2014; Yang et al., 2016). Note that, in this study, we only focus on the source-receptor relationships related to the wind anomalies during polluted days. In addition to winds, changes in other meteorological fields, such as precipitation, temperature, humidity, and planetary boundary layer height, could also influence the contributions of local aerosols between polluted and normal days. Although the BC emissions used in the simulation include a seasonal variability that could cause some variations in simulated concentrations, the monthly variability in DJF of BC emissions is less than 4% over China, which is negligible compared to the differences in concentrations between polluted and normal days.

4.3. Source contributions to trans-boundary and trans-Pacific transport

Considering the large contributions of emissions from South and Southeast Asia to MAM BC concentrations in the southwest China (Figure 6) and the large outflow of aerosols from East Asia in springtime (Yu et al., 2008), it is valuable to examine the inflow and outflow of BC in China. Figures S8a and S8b show the vertical distribution of source contributions of emissions from outside China to BC concentrations averaged over 75°–120°E and 25°–35°N, respectively, around the south boundary of continental China in MAM. High concentrations of BC originating from South and Southeast Asia are lifted to the free atmosphere in the south slope of Tibetan Plateau. Then westerly winds transport these BC particles to Southwest China and South China in both low- and mid-troposphere. Figures S8c and S8d present the contributions of emissions from China to BC concentrations averaged over 120°–135°E and 20°–50°N, respectively, around the east boundary of continental China. In MAM, the northward meridional winds over 25°–35°N and the southward meridional winds over 40°–50°N lead to the accumulation of BC in the lower atmosphere in eastern China. Westerly winds then transport these BC out of China mostly under 500 hPa.

Figure 10 shows the spatial distribution of column burden and surface concentrations of BC resulting from emissions in and outside China in MAM. Column burden is used to represent the outflow in this study following previous studies (Chin et al., 2007; Hadley et al., 2007). There are strong outflows across the Pacific Ocean originating from emissions both in and outside China. Emissions from China contribute 0.19 mg m^{-2} (or 53%) of MAM mean BC along 150°E averaged over 20°–60°N, whereas emissions outside China contribute 0.17 mg m^{-2} (or 47%). It suggests that both emissions from China and outside China are important for the outflow from East Asia. The yearly contribution from emissions from China to outflow from East Asia in this study is 58%, similar to the contribution of 61% in Matsui et al. (2013) calculated based on eastward BC mass flux using WRF-CMAQ model with INTEX-B missions. Averaged over western United States (125°–105°W, 30°–50°N), emissions from China account for 7% of near-surface BC concentrations and 25% in column burden in MAM, indicating that emissions from China could have a significant impact

on air quality in western United States. More than half of the China contribution to BC over western United States originates from eastern China (i.e., the tagged North and South China).

4.4. Source contributions to direct radiative forcing

The high concentrations of BC in China could also have a significant impact on the climate system through atmospheric heating or direct radiative forcing. As shown in Figure 11, the annual mean direct radiative forcing (DRF) of BC at TOA is as high as 3–4 W m^{-2} at some locations. Similar to the source attributions of BC concentrations (Figure 5) and burden (Figure S4), regional sources contribute the largest to DRF over the respective local regions. Among all the source regions in China, emissions from North, South, and Southwest China contribute the largest to local DRF of BC, with maximum DRF in a range of 3–5, 2–3, and 3–5 W m^{-2}, respectively. Other sources regions in China have relatively low contributions, with maximum values less than 2 W m^{-2}. Emissions outside China lead to 1–2 W m^{-2} of DRF of BC over South, Southwest, Northwest China and Tibetan Plateau, and 0.2–1 W m^{-2} over other parts of China, an effect that is quite widespread.

The total DRF of BC averaged over continental China simulated in this study is 2.27 W m^{-2}, larger than 0.64–1.55 W m^{-2} in previous studies (Wu et al., 2008; Zhuang et al., 2011; Li et al., 2016), probably due to the different emissions in the time periods of study, as shown in Table S5. Emissions outside China have the largest contributions to DRF of BC in China compared to any of the individual source regions in China, with an averaged contribution of 0.77 W m^{-2} (34%). This fractional contribution from emissions outside China is larger than 25% in Li et al. (2016), however we use different emissions, model and meteorology. Emissions from North China result in 0.56 W m^{-2} (25%) of DRF of BC over China, followed by 0.33 W m^{-2} (15%) and 0.31 W m^{-2} (14%) from South and Southwest China, respectively. Emissions from Central-West, Northeast, Northwest China, and Tibetan Plateau taken together account for 0.30 W m^{-2} (13%) of DRF of BC over China.

Yang Yang 1/18/2017 2:30 PM
Deleted: 75

Yang Yang 1/18/2017 2:30 PM
Deleted: 46

Yang Yang 1/18/2017 1:47 PM
Deleted: Zhuang et al., 2013;

Yang Yang 1/31/2017 4:33 PM
Deleted: The total BC emissions averaged over continental China were 1005 Gg C yr^{-1} for years 1993–2003 in Wu et al. (2008), 1811 Gg C yr^{-1} for year 2006 in Zhuang et al. (2011, 2013), and 1840 Gg C yr^{-1} for year 2010 in Li et al. (2016), whereas 2497 Gg C yr^{-1} for year 2010–2014 used in this study.

Yang Yang 1/31/2017 4:35 PM
Deleted: China

Figure 12a shows the seasonal mean DRF of BC averaged over China as a function of regional BC emissions. Because of high emissions, DRF of BC emitted from North China is the largest in all seasons, with values in a range of 0.5–0.7 W m^{-2} averaged over China, followed by 0.2–0.5 W m^{-2} from South and Southwest China. BC from the other tagged regions in China contribute less than 0.2 W m^{-2} in all seasons. In general, BC DRF in each season is proportional to its emission rate.

Figure 12b presents the seasonal DRF efficiency of BC emitted from the tagged regions and Table S6 summarizes these efficiencies. The variability of DRF efficiency for forcing over China is determined by several factors, such as incoming solar radiation (location of source regions), BC column burden and vertical distribution, and transport out of the region. The China DRF efficiency is largest in western China (NW and TP). This spatial pattern was also found by Henze et al. (2012). It can be explained by the increase of multiple scattering effects and attenuation of the transmitted radiation for large AOD (García et al., 2012). The Northeast China region has a low China DRF efficiency due to transport eastward outside of China. The remaining central and southern China regions have China DRF efficiencies that are fairly consistent, varying by 20-30% about the average. The annual mean and regional mean DRF efficiency in China is 0.91 W m^{-2} Tg^{-1}, within the range of 0.41–1.55 W m^{-2} Tg^{-1} from the previous studies (Table S5).

DRF efficiencies of BC from most regions have higher values in JJA and lower values in DJF. This is primarily due to more incoming solar radiation in summer. Insolation is the largest over Northwest China in JJA, together with less precipitation than other regions, resulting in large DRF efficiency there. Global BC DRF efficiency, particularly the annual average, is fairly similar for central, southern, and eastern China regions (Fig. 12c, d). Global efficiency is still much higher for the western regions.

BC emission reductions may impact mitigation of climate change and improve air quality. To compare the relative importance of climate and air quality effects of BC from different regions in China, Fig. 13 shows the near-surface concentration and column burden efficiency of BC over China and globally and Table S7 summarizes

these efficiencies. For near-surface concentration (Fig. 13a and 13b), the efficiencies are largest in DJF and lowest in JJA, in contrast to the DRF efficiencies, resulting from the less precipitation and wet deposition of aerosols in winter. Unlike the DRF efficiencies, the near-surface concentration efficiencies over eastern China are similar and even larger than those for central and western China. These results suggest that reduction in BC emissions in eastern China could benefit more on the regional air quality in China, especially in winter haze season.

The relative distributions of column burden efficiencies (Fig. 13c and 13d) are similar to the DRF efficiencies for the major emitting region in China, indicating that aerosol lifetime in atmosphere drives DRF that influences regional and global climate. The western regions (NW and TP), as expected, have a higher forcing per unit column burden.

5. Conclusions and discussions

In this study, the Community Earth System Model (CESM) with a source-tagging technique is used to quantify the contributions of BC emitted from seven regions in continental China, including North China (NC), South China (SC), Southwest China (SW), Central-West China (CW), Northeast China (NE), Northwest China (NW), and Tibetan Plateau (TP), and sources outside China (RW) to concentrations, haze formation, trans-boundary and trans-Pacific transport, and direct radiative forcing (DRF) of BC in China. The anthropogenic emissions of BC for years 2010-2014 used in this study were developed for the Coupled Model Intercomparison Project Phase 6 (CMIP6) from the Community Emissions Data System (CEDS). The annual total emission of BC from continental China is 2497 Gg C averaged over years 2010–2014. The model captures well the spatial distribution and seasonal variation in China. AAOD compares well with measurements, which are largely located in central and eastern China. Surface BC concentrations are underestimated by 53% compared to point observations.

The individual source regions are the largest contributors to their local BC concentration levels. Over North China where the air quality is often poor, about 90%

of near-surface BC concentration is contributed by local emissions. However, some source regions also impact BC in neighboring regions. Due to the seasonal variability of winds and emission rates, emissions from North China account for 30% of near-surface BC concentrations over South China in DJF (December-January-February), while emissions from outside China contribute about 10% in MAM (March-April-May). Over Southwest China, 17% of BC in MAM comes from sources outside China. Southwest and North China emissions contribute largely to BC in Central-West China. North China emissions have a contribution in a range of 12–36% to BC concentrations in Northeast China. Over Northwest China and Tibetan Plateau, more than 20% and 40% of BC, respectively, originates from emissions outside China. These indicate that, for regions with high emissions, their BC concentrations are dominated by local emissions. In contrast, BC levels over central and western China with lower emissions are more strongly influenced by non-local emissions. For all continental China as a whole, seasonal BC concentrations are largely due to emissions from North and South China, with relative contributions ranging from 43–50% and 18–24%, respectively, followed by contributions from Southwest (10–13%) and outside China (4–12%).

Emissions from non-local sources together with abnormal winds are one of the important factors contributing to high winter time pollution events in China. Over South China, about 50% of the increase in BC concentrations during high pollution conditions results from North China emissions. The increases in BC concentrations during polluted days over Southwest, Central-West and Northeast China are strongly influenced by emissions from eastern China. Emissions from outside China could contribute significantly to increases in BC concentrations over Northwest China and Tibetan Plateau during their polluted days. However, emissions from outside China do not have a significant contribution to haze in eastern and central China, suggesting that reduction in emissions within China would be needed to mitigate both local and non-local BC concentrations under high-polluted conditions.

Emissions from regions in and outside China both account for about half of BC outflow from East Asia, suggesting that emissions from China and other regions are

equally important for the BC outflow from East Asia. Through long-range transport, emissions from China result in 7% of near-surface BC concentration and 25% in column burden over western United States in MAM, indicating that emissions from China could have an impact on air quality in western United States.

The total DRF of BC averaged over continental China simulated in this study is 2.27 W m^{-2}. Among the tagged regions, emissions outside China have the largest single contribution to DRF of BC in China, with an average contribution of 34%, followed by 25%, 15%, and 14% due to emissions from North, South and Southwest China, respectively. DRF efficiencies over eastern China are small compared to central and western China in all seasons. For near-surface concentration, the efficiencies are largest in DJF and lowest in JJA, and efficiencies over eastern China are similar and even larger than central and western China. These suggest that reduction in BC emissions over eastern China could benefit more on the regional air quality in China, especially in winter haze season.

Note that the model largely underestimates BC concentrations over China, compared to the observation, which has also been reported in many previous studies using different models and different emission inventories (e.g., Liu et al., 2012; Fu et al., 2012; Huang et al., 2013; H. Wang et al., 2013; Q. Wang et al., 2014; R. Wang et al., 2014; Li et al., 2016). One possible reason is that in situ measurements are point observations, while the model does not treat the subgrid variability of aerosols and assumes aerosols are uniformly distributed over the grid cell. R. Wang et al. (2014) found a reduction of negative bias (from −88% to −35%) in the modeled surface BC concentrations when using high-resolution emissions and modeling at 0.5° X 0.7° resolution. This result indicates that the siting of observational stations can result in an artificial bias when comparing with relatively coarse model results. Further investigation of this siting/resolution bias is warranted, including investigation on whether this type of bias might extend, presumably to a lesser extent, also to AAOD measurements.

Further reasons that could contribute to this bias are emission underestimation or inaccurate aerosol processes in the model. Given that the differences between

Yang Yang 1/31/2017 4:48 PM
Deleted: are

Yang Yang 1/31/2017 4:49 PM
Deleted: It can be explained by the increase of multiple scattering effects and attenuation of the transmitted radiation for large AOD.

Yang Yang 1/31/2017 4:53 PM
Deleted: They find, however, that modeling over the North China Plain at an even higher resolution of 0.1°, further reduced the surface concentration bias there from 29% to 8%.

modeled and observed AAOD over eastern China are relatively small (–18%), we conclude that, given current evidence, the total amount of atmospheric BC in these simulations is reasonable at least in this sub-region.

Over eastern China, the BC concentrations are dominated by local emissions in this study, with local contribution of 64–93%. The underestimation of simulated BC concentrations over eastern China is more likely due to either underestimation of local emissions, too much aerosol removal within these regions, or resolution bias between observations and model grids. Over western China, 22–76% of the BC originates from emissions outside China. Thus biases of simulated BC concentrations could also come from underestimation of emissions outside China and or too much removal of BC during long-range transport. Satellite data are a promising method to validate modeling and emissions inventories, given that they do not depend on the location of observing stations, providing more uniform spatial coverage. A comparison of modeled AAOD and satellite AI provides an indication that the modeled burden in western China is underestimated, although the role of dust needs to be better characterized.

Uncertainty in China BC emissions has been estimated as –43% to 93% by Lu et al. (2011), –50% to 164% by Qin and Xie (2012), ±176% by Kurokawa et al. (2013), and –28 to 126% by Zhao et al. (2013). The BC emissions estimates used here for China in 2010 are 40% higher than those of Zhao et al. (2013) and Lu et al. (2011) and 30% higher than Klimont et al. (2016), in large part due to a higher estimate of BC emissions from coal coke production. Emissions from coke production are particularly uncertain given that "there are no measurements for $PM_{2.5}$ and BC emissions" (Huo et al. 2012) available to guide inventory estimates. Total rest of the world emissions other than China, which appear to be a major contributor to burdens over western regions, are within 1% of those from Klimont et al. (2016).

BC aging in the atmosphere is important for BC concentration and its optical properties, which transforms BC from hydrophobic aggregates to hydrophilic particles coated with soluble materials. He et al. (2015, 2016a) found that BC optical properties varied by a factor of two or more due to different coating structures during BC aging

Yang Yang 1/31/2017 4:55 PM
Deleted: aerosol index (

Yang Yang 1/31/2017 4:55 PM
Deleted:)

Hailong Wang 2/1/2017 12:23 PM
Deleted: up to more than

process based on their theoretical and experimental intercomparison. Oshima et al. (2009) and He et al. (2016b) pointed out that the use of various microphysical BC aging schemes could significantly improve simulations of BC concentrations, compared to the simplified aging parameterizations. Liu et al. (2012) also reported that the wet removal rate of BC simulated in standard CAM5 is 60% higher than AeroCom multi-model mean due to the rapid or instantaneous aging of BC. H. Wang et al. (2013) showed that the explicit treatment of BC aging process with slow aging assumptions in CAM5 could significantly increase BC lifetime and the efficiency of BC long-range transport. In the three-mode aerosol module (MAM3) of CAM5 used in this study, the aging process of BC is neglected by assuming the immediate internal mixing of BC with other aerosol species in the same mode. This assumption could lead to an overestimation of wet removal of BC and, therefore, an underestimation of BC concentrations, absorption optical depth (Fig. 3) and direct radiative forcing. In addition, the internally-mixed optical treatment in CAM5 could also cause bias in BC absorption calculation. However, H. Wang et al. (2014) examined source-receptor relationships for BC under the different BC aging assumptions and found that the quantitative source attributions varied slightly while the qualitative source-receptor relationships still hold. Therefore, although the magnitude of simulated BC and its optical properties could be underestimated due to the instantaneous aging of BC and uncertainty in coating structures, we expect that the aging treatment in MAM3 of CAM5 should not influence the qualitative source attributions examined in this study.

In this study, BC is used as an indicator of pollution (or air quality) in China. Although BC is often co-emitted with other species, such as primary organic matter, organic gases and sulfuric gases, source-receptor relationship of BC may not fully represent that of total aerosols. The contribution of BC to total near-surface $PM_{2.5}$ concentrations averaged over China is less than 10%. Other aerosols, such as sulfate, are dominant in China during polluted days. The spatio-temporal variations and source contributions of these species are largely different from those of BC because spatial distributions of emissions (e.g., SO_2) and formation processes can be considerably different. For example, Matsui et al. (2009) showed that primary

aerosols around Beijing were determined by emissions within 100 km around Beijing within the preceding 24 hours, while emissions as far as 500 km and within the preceding 3 days were found to affect secondary aerosols in Beijing. Thus, the secondary aerosols could have larger contributions from non-local emissions than BC. BC concentrations are highest in winter over China due to higher emissions, while sulfate concentrations reach maximum in summer when the strong sunlight and high temperature favor the sulfate formation. Therefore, knowing the accurate source attributions of air pollution in China requires source tagging for more aerosol species, such as sulfate.

Acknowledgments.

This research was supported by the National Atmospheric and Space Administration's Atmospheric Composition: Modeling and Analysis Program (ACMAP), award NNH15AZ64I. We also acknowledge additional support from the U.S. Department of Energy (DOE), Office of Science, Biological and Environmental Research. The Pacific Northwest National Laboratory is operated for DOE by Battelle Memorial Institute under contract DE-AC05-76RLO1830. The CESM project was supported by the National Science Foundation and the DOE Office of Science. The satellite-derived Total Ozone Mapping Spectromenter Aerosol Index monthly data sets are obtained from the Web site at http://disc.sci.gsfc.nasa.gov/data-holdings/PIP/aerosol_index.shtml. The National Energy Research Scientific Computing Center (NERSC) provided computational resources. Model results are available through NERSC upon request.

References

Abdul-Razzak, H., and Ghan, S. J.: A parameterization of aerosol activation: 2. Multiple aerosol types, J. Geophys. Res., 105, 6837–6844, doi:10.1029/1999JD901161, 2000.

Anenberg, S. C., Talgo, K., Arunachalam, S., Dolwick, P., Jang, C., and West, J. J.: Impacts of global, regional, and sectoral black carbon emission reductions on surface air quality and human mortality, Atmos. Chem. Phys., 11, 7253-7267, doi:10.5194/acp-11-7253-2011, 2011.

Bond, T. C., Streets, D. G., Yarber, K. F., Nelson, S. M., Woo, J.-H., and Klimont, Z.: A technology-based global inventory of black and organic carbon emissions from combustion, J. Geophys. Res., 109, D14203, doi:10.1029/2003JD003697, 2004.

Bond, T. C., and Bergstrom, R. W.: Light absorption by carbonaceous particles: An investigative review, Aerosol. Sci. Technol., 40, 27–67, doi:10.1080/02786820500421521, 2006.

Bond, T. C., Bhardwaj, E., Dong, R., Jogani, R., Jung, S., Roden, C., Streets, D. G., and Trautmann, N. M.: Historical emissions of black and organic carbon aerosol from energy-related combustion, 1850–2000, Global Biogeochem. Cycles, 21, GB2018, doi:10.1029/2006GB002840, 2007.

1828 Bond, T. C., Doherty, S. J., Fahey, D. W., Forster, P. M., Berntsen, T., DeAngelo,B.
1829 J., Flanner, M. G., Ghan, S., Kärcher, B., Koch, D., Kinne, S., Kondo, Y., Quinn,
1830 P. K., Sarofim, M. C., Schultz, M. G., Schulz, M., Venkataraman, C., Zhang, H.,
1831 Zhang, S., Bellouin, N., Guttikunda, S. K., Hopke, P. K., Jacob- son, M. Z.,
1832 Kaiser, J. W., Klimont, Z., Lohmann, U., Schwarz, J. P., Shindell, D., Storelvmo,
1833 T., Warren, S. G., and Zender, C. S.: Bounding the role of black carbon in the
1834 climate sys- tem: A scientific assessment, J. Geophys. Res., 118, 5380–5552,
1835 doi:10.1002/jgrd.50171, 2013.
1836
1837 Chin, M., Diehl, T., Ginoux, P., and Malm, W.: Intercontinental transport of pollution
1838 and dust aerosols: implications for regional air quality, Atmos. Chem. Phys., 7,
1839 5501-5517, doi:10.5194/acp-7-5501-2007, 2007.
1840
1841 Ding, Y. H., and Liu, Y. J.: Analysis of long-term variations of fog and haze in China in
1842 recent 50 years and their relations with atmospheric humidity, Sci. China Earth
1843 Sci., 57, 36–46, doi:10.1007/s11430-013-4792-1, 2014.
1844
1845 Flanner, M. G., Zender, C. S., Randerson, J. T., and Rasch, P. J.: Present day
1846 climate forcing and response from black carbon in snow, J. Geophys. Res., 112,
1847 D11202, doi:10.1029/2006JD008003, 2007.
1848

1849 Fu, T.-M., Cao, J. J., Zhang, X. Y., Lee, S. C., Zhang, Q., Han, Y. M., Qu, W. J., Han,
1850 Z., Zhang, R., Wang, Y. X., Chen, D., and Henze, D. K.: Carbonaceous aerosols
1851 in China: top-down constraints on primary sources and estimation of secondary
1852 contribution, Atmos. Chem. Phys., 12, 2725-2746,
1853 doi:10.5194/acp-12-2725-2012, 2012.
1854
1855 García, O. E., Díaz, J. P., Expósito, F. J., Díaz, A. M., Dubovik, O., Derimian, Y.,
1856 Dubuisson, P., and Roger, J.-C.: Shortwave radiative forcing and efficiency of key
1857 aerosol types using AERONET data, Atmos. Chem. Phys., 12, 5129-5145,
1858 doi:10.5194/acp-12-5129-2012, 2012.
1859
1860 Ghan, S. J., and Zaveri, R. A.: Parameterization of optical properties for hydrated
1861 internally mixed aerosol, J. Geophys. Res., 112, D10201,
1862 doi:10.1029/2006JD007927, 2007.
1863
1864 Ghan, S. J., Technical Note: Estimating aerosol effects on cloud radiative forcing,
1865 Atmos. Chem. Phys., 13, 9971-9974, doi:10.5194/acp-13-9971-2013, 2013.
1866
1867 Hadley, O. L., Ramanathan, V., Carmichael, G. R., Tang, Y., Corrigan, C. E.,
1868 Roberts, G. C., and Mauger, G. S.: Trans-Pacific transport of black carbon and
1869 fine aerosols (D < 2.5 μm) into North America, J. Geophys. Res., 112, D05309,
1870 doi:10.1029/2006JD007632, 2007.

He, C., Liou, K.-N., Takano, Y., Zhang, R., Levy Zamora, M., Yang, P., Li, Q., and Leung, L. R.: Variation of the radiative properties during black carbon aging: theoretical and experimental intercomparison, Atmos. Chem. Phys., 15, 11967-11980, doi:10.5194/acp-15-11967-2015, 2015.

He, C., Takano, Y., Liou, K.-N., Yang, P., Li, Q., and Mackowski, D. W.: Intercomparison of the GOS approach, superposition T- matrix method, and laboratory measurements for black carbon optical properties during aging, J. Quant. Spectrosc. Ra., 184, 287–296, doi:10.1016/j.jqsrt.2016.08.004, 2016a.

He, C., Li, Q., Liou, K.-N., Qi, L., Tao, S., and Schwarz, J. P.: Microphysics-based black carbon aging in a global CTM: constraints from HIPPO observations and implications for global black carbon budget, Atmos. Chem. Phys., 16, 3077-3098, doi:10.5194/acp-16-3077-2016, 2016b.

Henze, D. K., Shindell, D. T., Akhtar, F., R. Spurr, J. D., Pinder, R. W., Loughlin, D., Kopacz, M., Singh, K., and Shim, C.: Spatially refined aerosol direct radiative forcing efficiencies, Environ. Sci. Technol., 46, 9511–9518, doi:10.1021/es301993s, 2012.

Holben, B. N., Tanré, D., Smirnov, A., Eck, T. F., Slutsker, I., Abuhassan, N., Newcomb, W. W., Schafer, J. S., Chatenet, B., Lavenu, F., Kaufman, Y. J., Castle, J. V., Setzer, A., Markham, B., Frouin, D. C. R., Halthore, R., Karneli, A., O'Neill, N. T., Pietras, C., Pinker, R. T., Voss, K., and Zibordi, G.: An emerging ground-based aerosol climatology: Aerosol optical depth from AERONET, J. Geophys. Res., 106, 12 067–12 098, 2001.

Huang, Y., Wu, S., Dubey, M. K., and French, N. H. F.: Impact of aging mechanism on model simulated carbonaceous aerosols, Atmos. Chem. Phys., 13, 6329-6343, doi:10.5194/acp-13-6329-2013, 2013.

Huo, H., Lei, Y., Zhang, Q., Zhao, L. J., and He, K. B.: China's coke industry: Recent policies, technology shift, and implication for energy and the environment, Energ. Policy., 51, 397–404, doi:10.1016/j.enpol.2012.08.041, 2012.

Hurrell, J. W., Holland, M. M., Gent, P. R., Ghan, S., Kay, J. E., Kushner, P. J., Lamarque, J. F., Large, W. G., Lawrence, D., Lind- say, K., Lipscomb, W. H., Long, M. C., Mahowald, N., Marsh, D. R., Neale, R. B., Rasch, P., Vavrus, S., Vertenstein, M., Bader, D., Collins, W. D., Hack, J. J., Kiehl, J., and Marshall, S.: The Community Earth System Model A Framework for Collabora- tive Research, B. Am. Meteorol. Soc., 94, 1339–1360, 2013.

IPCC, 2013, Climate Change 2013: the Physical Science Basis. Contribution of Working Group I to the Fifth Assessment Report of the Intergovernmental Panel on Climate Change. Cambridge University Press, Cambridge, United Kingdom and New York, NY, USA, p. 1535.

Jacobson, M. Z.: Effects of externally-through-internally-mixed soot inclusions within clouds and precipitation on global climate, J. Phys. Chem. A, 110, 6860–6873, doi:10.1021/Jp056391r, 2006.

Janssen, N. A. H., Gerlofs-Nijiland, M. E., Lanki, T., Salonen, R. O., Cassee, F., Hoek, G., Fischer, P., Brunekreef, B., and Krzyzanowski, M.: Health Effects of Black Carbon, World Health Organization, Copenhagen, 2012.

Janssens-Maenhout, G., Crippa, M., Guizzardi, D., Dentener, F., Muntean, M., Pouliot, G., Keating, T., Zhang, Q., Kurokawa, J., Wankmüller, R., Denier van der Gon, H., Kuenen, J. J. P., Klimont, Z., Frost, G., Darras, S., Koffi, B., and Li, M.: HTAP_v2.2: a mosaic of regional and global emission grid maps for 2008 and 2010 to study hemispheric transport of air pollution, Atmos. Chem. Phys., 15, 11411-11432, doi:10.5194/acp-15-11411-2015, 2015.

Jiao, C., Flanner, M. G., Balkanski, Y., Bauer, S. E., Bellouin, N., Berntsen, T. K., Bian, H., Carslaw, K. S., Chin, M., De Luca, N., Diehl, T., Ghan, S. J., Iversen, T.,

1936 Kirkevåg, A., Koch, D., Liu, X., Mann, G. W., Penner, J. E., Pitari, G., Schulz, M.,
1937 Seland, Ø., Skeie, R. B., Steenrod, S. D., Stier, P., Takemura, T., Tsigaridis, K.,
1938 van Noije, T., Yun, Y., and Zhang, K.: An AeroCom assessment of black carbon
1939 in Arctic snow and sea ice, Atmos. Chem. Phys., 14, 2399-2417,
1940 doi:10.5194/acp-14-2399-2014, 2014.
1941
1942 Klimont, Z., Kupiainen, K., Heyes, C., Purohit, P., Cofala, J., Rafaj, P.,
1943 Borken-Kleefeld, J., and Schöpp, W.: Global anthropogenic emissions of
1944 particulate matter including black carbon, Atmos. Chem. Phys. Discuss.,
1945 doi:10.5194/acp-2016-880, in review, 2016.
1946
1947 Koepke, M. H. P., and Schult, I.: Optical properties of aerosols and clouds: The
1948 software package opac, Bull. Am. Meteorol. Soc., 79, 831–844,
1949 doi:10.1175/1520-0477(1998)079<0831:OPOAAC>2.0.CO;2, 1998.
1950
1951 Kristiansen, N. I., Stohl, A., Olivié, D. J. L., Croft, B., Søvde, O. A., Klein, H.,
1952 Christoudias, T., Kunkel, D., Leadbetter, S. J., Lee, Y. H., Zhang, K., Tsigaridis,
1953 K., Bergman, T., Evangeliou, N., Wang, H., Ma, P.-L., Easter, R. C., Rasch, P. J.,
1954 Liu, X., Pitari, G., Di Genova, G., Zhao, S. Y., Balkanski, Y., Bauer, S. E.,
1955 Faluvegi, G. S., Kokkola, H., Martin, R. V., Pierce, J. R., Schulz, M., Shindell, D.,
1956 Tost, H., and Zhang, H.: Evaluation of observed and modelled aerosol lifetimes

using radioactive tracers of opportunity and an ensemble of 19 global models, Atmos. Chem. Phys., 16, 3525-3561, doi:10.5194/acp-16-3525-2016, 2016.

Kurokawa, J., Ohara, T., Morikawa, T., Hanayama, S., Janssens-Maenhout, G., Fukui, T., Kawashima, K., and Akimoto, H.: Emissions of air pollutants and greenhouse gases over Asian regions during 2000–2008: Regional Emission inventory in ASia (REAS) version 2, Atmos. Chem. Phys., 13, 11019-11058, doi:10.5194/acp-13-11019-2013, 2013.

Lau, K.-M., Kim, M. K., Kim, K.-M., and Lee, W. S.: Enhanced surface warming and accelerated snow melt in the Himalayas and Tibetan Plateau induced by absorbing aerosols, Environ. Res. Lett., 5, 025204, doi:10.1088/1748-9326/5/2/025204, 2010.

Li, K., Liao, H., Mao, Y. H., and Ridley, D. A.: Source sector and region contributions to concentration and direct radiative forcing of black carbon in China, Atmos. Environ., 124, 351–366, doi:10.1016/j.atmosenv.2015.06.014, 2016.

Liao, H., Chang, W. Y., and Yang, Y.: Climatic effects of air pollutants over China: A review, Adv. Atmos. Sci., 32, 115–139, doi:10.1007/s00376-014-0013-x, 2015.

Liu, X., Easter, R. C., Ghan, S. J., Zaveri, R., Rasch, P., Shi, X., Lamarque, J.-F., Gettelman, A., Morrison, H., Vitt, F., Conley, A., Park, S., Neale, R., Hannay, C., Ekman, A. M. L., Hess, P., Mahowald, N., Collins, W., Iacono, M. J., Bretherton, C. S., Flanner, M. G., and Mitchell, D.: Toward a minimal representation of aerosols in climate models: description and evaluation in the Community Atmosphere Model CAM5, Geosci. Model Dev., 5, 709-739, doi:10.5194/gmd-5-709-2012, 2012.

Liu, X., Ma, P.-L., Wang, H., Tilmes, S., Singh, B., Easter, R. C., Ghan, S. J., and Rasch, P. J.: Description and evaluation of a new four-mode version of the Modal Aerosol Module (MAM4) within version 5.3 of the Community Atmosphere Model, Geosci. Model Dev., 9, 505-522, doi:10.5194/gmd-9-505-2016, 2016.

Lou, S., Russell, L. M., Yang, Y., Xu, L., Lamjiri, M. A., DeFlorio, M. J., Miller, A. J., Ghan, S. J., Liu, Y., and Singh, B.: Impacts of the East Asian Monsoon on springtime dust concentrations over China, J. Geophys. Res. Atmos., 121, 8137–8152, doi:10.1002/2016JD024758, 2016.

Lu, Z., Zhang, Q., and Streets, D. G.: Sulfur dioxide and primary carbonaceous aerosol emissions in China and India, 1996–2010, Atmos. Chem. Phys., 11, 9839-9864, doi:10.5194/acp-11-9839-2011, 2011.

2000 Ma, P.-L., Gattiker, J. R., Liu, X., and Rasch, P. J.: A novel approach for determining
2001 source-receptor relationships in model simulations: a case study of black carbon
2002 transport in northern hemisphere winter, Environ. Res. Lett., 8(2), 024042,
2003 doi:10.1088/1748-9326/8/2/024042, 2013a.
2004
2005 Ma, P.-L., Rasch, P. J., Wang, H., Zhang, K., Easter, R. C., Tilmes, S., Fast, J. D.,
2006 Liu, X., Yoon, J.-H., and Lamarque, J.-F.: The role of circulation features on black
2007 carbon transport into the Arctic in the Community Atmosphere Model version 5
2008 (CAM5), J. Geophys. Res. Atmos., 118, 4657–4669, doi:10.1002/jgrd.50411,
2009 2013b.
2010
2011 Matsui, H., Koike, M., Kondo, Y., Takegawa, N., Kita, K., Miyazaki, Y., Hu, M., Chang,
2012 S.-Y., Blake, D. R., Fast, J. D., Zaveri, R. A., Streets, D. G., Zhang, Q., and Zhu,
2013 T.: Spatial and temporal variations of aerosols around Beijing in summer 2006:
2014 Model evaluation and source apportionment, J. Geophys. Res., 114, D00G13,
2015 doi:10.1029/2008JD010906, 2009.
2016
2017 Matsui, H., Koike, M., Kondo, Y., Oshima, N., Moteki, N., Kanaya, Y., Takami, A., and
2018 Irwin, M.: Seasonal variations of Asian black carbon outflow to the Pacific:
2019 Contribution from anthropogenic sources in China and biomass burning sources
2020 in Siberia and Southeast Asia, J. Geophys. Res. Atmos., 118, 9948–9967,
2021 doi:10.1002/jgrd.50702, 2013.

McFarquhar, G., and Wang, H.: Effects of aerosols on trade wind cumuli over the Indian Ocean: Model simulations, Q. J. R. Meteorol. Soc., 132, 821–843, doi:10.1256/qj.04.179, 2006.

Oshima, N., Koike, M., Zhang, Y., Kondo, Y., Moteki, N., Takegawa, N., and Miyazaki, Y.: Aging of black carbon in outflow from anthropogenic sources using a mixing state resolved model: Model development and evaluation, J. Geophys. Res., 114, D06210, doi:10.1029/2008JD010680, 2009.

Oshima, N., Kondo, Y., Moteki, N., Takegawa, N., Koike, M., Kita, K., Matsui, H., Kajino, M., Nakamura, H., Jung, J. S., and Kim, Y. J.: Wet removal of black carbon in Asian outflow: Aerosol Radiative Forcing in East Asia (A-FORCE) aircraft campaign, J. Geophys. Res., 117, D03204, doi:10.1029/2011jd016552, 2012.

Qian, Y., Flanner, M. G., Leung, L. R., and Wang, W.: Sensitivity studies on the impacts of Tibetan Plateau snowpack pollution on the Asian hydrological cycle and monsoon climate, Atmos. Chem. Phys., 11, 1929-1948, doi:10.5194/acp-11-1929-2011, 2011.

2043 Qian, Y., Wang, H., Zhang, R., Flanner, M. G., and Rasch, P. J.: A sensitivity study on
2044 modeling black carbon in snow and its radiative forcing over the Arctic and
2045 Northern China, Environ. Res. Lett., 9, 064001,
2046 doi:10.1088/1748-9326/9/6/064001, 2014.
2047
2048 Qian, Y., Yasunari, T. J., Doherty, S. J., Flanner, M. G., Lau, W. K. M., Ming, J.,
2049 Wang, H., Wang, M., Warren, S. G., and Zhang, R.: Light-absorbing particles in
2050 snow and ice: Measurement and modeling of climatic and hydrological impact,
2051 *Adv. Atmos. Sci.*, 32(1), 64–91, doi:10.1007/s00376-014-0010-0, 2015.
2052
2053 Qin, Y. and Xie, S. D.: Spatial and temporal variation of anthropogenic black carbon
2054 emissions in China for the period 1980–2009, Atmos. Chem. Phys., 12,
2055 4825-4841, doi:10.5194/acp-12-4825-2012, 2012.
2056
2057 Ramanathan, V., and Carmichael, G.: Global and regional climate changes due to
2058 black carbon, Nat. Geosci., 1, 221-227, doi:10.1038/ngeo156, 2008.
2059
2060 Rienecker, M. M., Suarez, M. J., Gelaro, R., Todling, R., Bacmeis- ter, J., Liu, R.,
2061 Bosilovich, M. G., Schubert, S. D., Takacs, L., Kim, G-K, Bloom, S., Chen, J.,
2062 Collins, D., Conaty, A., da Silva, A., Gu, W., Joiner, J., Koster, R. D., Lucchesi,
2063 R., Molod, A., Owens, T., Pawson, S., Pegion, P., Redder, C. R., Reichle, R.,
2064 Robertson, F. R., Ruddick, A. G., Sienkiewicz, M., and Woollen, J.: MERRA:

2065 NASA's Modern-Era Retrospective Analysis for Research and Applications, J.
2066 Climate, 24, 3624–3648, 2011.
2067
2068 Schuster, G. L., Dubovik, O., Arola, A., Eck, T. F., and Holben, B. N.: Remote sensing
2069 of soot carbon – Part 2: Understanding the absorption Ångström exponent,
2070 Atmos. Chem. Phys., 16, 1587-1602, doi:10.5194/acp-16-1587-2016, 2016.
2071
2072 Shindell, D., et al. (2012), Simultaneously mitigating near-term climate change and
2073 improving human health and food security, Science, 335(6065), 183-189,
2074 doi:10.1126/science.1210026.
2075
2076 Shindell, D., Kuylenstierna, J. C. I., Vignati, E., van Dingenen, R., Amann, M.,
2077 Klimont, Z., Anenberg, S. C., Muller, N., Janssens- Maenhout, G., Raes, F.,
2078 Schwartz, J., Faluvegi, G., Pozzoli, L., Kupiainen, K., Höglund-Isaksson, L.,
2079 Emberson, L., Streets, D., Ramanathan, V., Hicks, K., Oanh, N. T. K., Milly, G.,
2080 Williams, M., Demkine, V., and Fowler, D.: Simultaneously Mitigating Near-Term
2081 Climate Change and Improving Human Health and Food Security, Science, 335,
2082 183–189, doi:10.1126/science.1210026, 2012.
2083
2084 Smith, S. J., and Mizrahi, A.: Near-term climate mitigation by short-lived forcers, Proc.
2085 Natl. Acad. Sci, 110(35), 14202-14206, doi:10.1073/pnas.1308470110, 2013.
2086

2087 Sun, Y., Jiang, Q., Wang, Z., Fu, P., Li, J., Yang, T., and Yin, Y.: Investigation of the
2088 sources and evolution processes of severe haze pollution in Beijing in January
2089 2013, J. Geophys. Res. Atmos., 119, 4380–4398, doi:10.1002/2014JD021641,
2090 2014.
2091
2092 Wang, H., Easter, R. C., Rasch, P. J., Wang, M., Liu, X., Ghan, S. J., Qian, Y., Yoon,
2093 J.-H., Ma, P.-L., and Vinoj, V.: Sensitivity of remote aerosol distributions to
2094 representation of cloud–aerosol interactions in a global climate model, Geosci.
2095 Model Dev., 6, 765-782, doi:10.5194/gmd-6-765-2013, 2013.
2096
2097 Wang, H., Rasch, P. J., Easter, R. C., Singh, B., Zhang, R., Ma, P.-L., Qian, Y., Ghan,
2098 S. J., and Beagley, N.: Using an explicit emission tagging method in global
2099 modeling of source-receptor relationships for black carbon in the Arctic:
2100 Variations, sources, and transport pathways, J. Geophys. Res. Atmos., 119,
2101 12,888–12,909, doi:10.1002/ 2014JD022297, 2014.
2102
2103 Wang, L. T., Wei, Z., Yang, J., Zhang, Y., Zhang, F. F., Su, J., Meng, C. C., and
2104 Zhang, Q.: The 2013 severe haze over southern Hebei, China: model evaluation,
2105 source apportionment, and policy implications, Atmos. Chem. Phys., 14,
2106 3151-3173, doi:10.5194/acp-14-3151-2014, 2014.
2107

Wang, M., Ghan, S., Ovchinnikov, M., Liu, X., Easter, R., Kassianov, E., Qian, Y., and Morrison, H.: Aerosol indirect effects in a multi-scale aerosol-climate model PNNL-MMF, Atmos. Chem. Phys., 11, 5431-5455, doi:10.5194/acp-11-5431-2011, 2011.

Wang, Q., Jacob, D. J., Spackman, J. R., Perring, A. E., Schwarz, J. P., Moteki, N., Marais, E. A., Ge, C., Wang, J., and Bar- rett, S. R. H.: Global budget and radiative forcing of black car- bon aerosol: Constraints from pole-to-pole (HIPPO) observa- tions across the Pacific, J. Geophys. Res.-Atmos., 119, 195–206, doi:10.1002/2013jd020824, 2014.

Wang, R., Tao, S., Balkanski, Y., Ciais, P., Boucher, O., Liu, J., Piao, S., Shen, H., Vuolo, M. R., and Valari, M.: Exposure to ambient black carbon derived from a unique inventory and high- resolution model, P. Natl. Acad. Sci. USA, 111, 2459–2463, 2014.

Wang, X., Wang, Y., Hao, J., Kondo, Y., Irwin, M., Munger, J. W., and Zhao, Y.: Top-down estimate of China's black carbon emissions using surface observations: Sensitivity to observation representativeness and transport model error, J. Geophys. Res. Atmos., 118, 5781–5795, doi:10.1002/jgrd.50397, 2013.

Wu, J., Fu, C., Xu, Y., Tang, J. P., Wang, W., and Wang, Z.: Simulation of direct effects of black carbon aerosol on temperature and hydrological cycle in Asia by a Regional Climate Model, Meteorol. Atmos. Phys., 100(1), 179–193, doi:10.1007/s00703-008-0302-y, 2008.

Yang, Y., Liao, H., and Lou, S.: Decadal trend and interannual variation of outflow of aerosols from East Asia: Roles of variations in meteorological parameters and emissions, Atmos. Environ., 100, 141-153, doi:10.1016/j.atmosenv.2014.11.004, 2015.

Yang, Y., Liao, H., and Lou, S.: Increase in winter haze over eastern China in recent decades: Roles of variations in meteorological parameters and anthropogenic emissions, J. Geophys. Res. Atmos., 121, doi:10.1002/2016JD025136, 2016.

Yu, H., Remer, L. A., Chin, M., Bian, H., Kleidman, R. G., and Diehl, T.: A satellite-based assessment of transpacific transport of pollution aerosol, J. Geophys. Res., 113, D14S12, doi:10.1029/2007JD009349, 2008.

Zhang, K., Wan, H., Liu, X., Ghan, S. J., Kooperman, G. J., Ma, P.-L., Rasch, P. J., Neubauer, D., and Lohmann, U.: Technical Note: On the use of nudging for aerosol–climate model intercomparison studies, Atmos. Chem. Phys., 14, 8631-8645, doi:10.5194/acp-14-8631-2014, 2014.

Zhang, L. M., Gong, S. L., Padro, J., and Barrie, L.: A size-segregated particle dry deposition scheme for an atmospheric aerosol module, Atmos. Environ., 35, 549-560, doi:10.1016/S1352-2310(00)00326-5, 2001.

Zhang, Q., Streets, D. G., Carmichael, G. R., He, K. B., Huo, H., Kannari, A., Klimont, Z., Park, I. S., Reddy, S., Fu, J. S., Chen, D., Duan, L., Lei, Y., Wang, L. T., and Yao, Z. L.: Asian emissions in 2006 for the NASA INTEX-B mission, Atmos. Chem. Phys., 9, 5131-5153, doi:10.5194/acp-9-5131-2009, 2009.

Zhang, R. H., Li, Q., and Zhang, R. N.: Meteorological conditions for the persistent severe fog and haze event over eastern China in January 2013, Sci. China Earth Sci., 57(1), 26–35, doi:10.1007/s11430-013-4774-3, 2014.

Zhang, R., Wang, H., Hegg, D. A., Qian, Y., Doherty, S. J., Dang, C., Ma, P.-L., Rasch, P. J., and Fu, Q.: Quantifying sources of black carbon in western North America using observationally based analysis and an emission tagging technique in the Community Atmosphere Model, Atmos. Chem. Phys., 15, 12805-12822, doi:10.5194/acp-15-12805-2015, 2015a.

Zhang, R., Wang, H., Qian, Y., Rasch, P. J., Easter, R. C., Ma, P.-L., Singh, B., Huang, J., and Fu, Q.: Quantifying sources, transport, deposition, and radiative

forcing of black carbon over the Himalayas and Tibetan Plateau, Atmos. Chem. Phys., 15, 6205-6223, doi:10.5194/acp-15-6205-2015, 2015b.

Zhang, X. Y., Wang, Y. Q., Zhang, X. C., Guo, W., and Gong, S. L.: Carbonaceous aerosol composition over various regions of China during 2006, J. Geophys. Res., 113, D14111, doi:10.1029/2007JD009525, 2008.

Zhang, X. Y., Wang, Y. Q., Niu, T., Zhang, X. C., Gong, S. L., Zhang, Y. M., and Sun, J. Y.: Atmospheric aerosol compositions in China: spatial/temporal variability, chemical signature, regional haze distribution and comparisons with global aerosols, Atmos. Chem. Phys., 12, 779-799, doi:10.5194/acp-12-779-2012, 2012.

Zhang, Y.-L., Huang, R.-J., El Haddad, I., Ho, K.-F., Cao, J.-J., Han, Y., Zotter, P., Bozzetti, C., Daellenbach, K. R., Canonaco, F., Slowik, J. G., Salazar, G., Schwikowski, M., Schnelle-Kreis, J., Abbaszade, G., Zimmermann, R., Baltensperger, U., Prévôt, A. S. H., and Szidat, S.: Fossil vs. non-fossil sources of fine carbonaceous aerosols in four Chinese cities during the extreme winter haze episode of 2013, Atmos. Chem. Phys., 15, 1299-1312, doi:10.5194/acp-15-1299-2015, 2015.

2194 Zhao, Y., Zhang, J., and Nielsen, C. P.: The effects of recent control policies on
2195 trends in emissions of anthropogenic atmospheric pollutants and CO2 in China,
2196 Atmos. Chem. Phys., 13, 487-508, doi:10.5194/acp-13-487-2013, 2013.
2197
2198 Zhuang, B. L., Jiang, F., Wang, T. J., Li, S., and Zhu, B.: Investigation on the direct
2199 radiative effect of fossil fuel black-carbon aerosol over China, Theor. Appl.
2200 Climatol., 104(3), 301–312, doi:10.1007/s00704-010-0341-4, 2011.
2201
2202 Zhuang, B. L., Liu, Q., Wang, T. J., Yin, C. Q., Li, S., Xie, M., Jiang, F., and Mao, H.
2203 T.: Investigation on semi-direct and indirect climate effects of fossil fuel black
2204 carbon aerosol over China, Theor. Appl. Climatol., 114 (3), 651–672,
2205 doi:10.1007/s00704-013-0862-8, 2013.
2206
2207 Zhuang, B. L., Wang, T. J., Liu, J., Li, S., Xie, M., Yang, X. Q., Fu, C. B., Sun, J. N.,
2208 Yin, C. Q., Liao, J. B., Zhu, J. L., and Zhang, Y.: Continuous measurement of
2209 black carbon aerosol in urban Nanjing of Yangtze River Delta, China, Atmos.
2210 Environ., 89, 415–424, doi:10.1016/j.atmosenv.2014.02.052, 2014.
2211
2212
2213
2214

Figure Captions

Figure 1. (a) Spatial distribution of annual mean total emissions (anthropogenic plus biomass burning, units: g C m^{-2} yr^{-1}) of black carbon (BC) averaged over 2010–2014. The geographical BC source regions are selected as North China (NC, 109°E–east boundary, 30°–41°N), South China (SC, 109°E–east boundary, south boundary–30°N), Southwest China (SW, 100°–109°N, south boundary–32°N), Central-West China (CW, 100°–109°N, 32°N–north boundary), Northeast China (NE, 109°E–east boundary, 41°N–north boundary), Northwest China (NW, west boundary–100°E, 36°N–north boundary), and Tibetan Plateau (TP, west boundary–100°E, south boundary–36°N) in China and regions outside of China (RW, rest of the world). (b) Seasonal mean total emissions (units: Gg C, Gg = 10^9g) of BC from the seven BC source regions in China and emissions from rest of East Asia (REA, with China excluded), South Asia (SAS), Southeast Asia (SEA), and Russia/Belarussia/Ukraine (RBU).

Figure 2. Simulated seasonal mean near-surface concentrations (left, units: μg m^{-3}) and column burden (right, units: mg m^{-2}) of BC in December-January-February (DJF), March-April-May (MAM), June-July-August (JJA), and September-October-November (SON).

Figure 3. Comparisons of observed and modeled seasonal mean (a) near-surface concentrations (units: μg m^{-3}) and (b) aerosol absorption optical depth (AAOD) of BC in China. Solid lines mark the 1:1 ratios and dashed lines mark the 1:3 and 3:1 ratios. Observed BC concentrations were taken between 2006 and 2007 at 14 sites of the China Meteorological Administration (CMA) Atmosphere Watch Network (CAWNET) (Zhang et al., 2012). Observed AAOD of BC are obtained by removing dust AAOD from total AAOD at 10 sites of the Aerosol Robotic Network (AERONET) (Holben et al., 2001), following Bond et al. (2013). The observed AAOD are averaged over years of 2005–2014 with data available. Correlation coefficient (R) and normalized mean

bias (NMB) between observation and simulation are shown on top left of each panel. NMB = 100%× $\sum(M_i - O_i) / \sum O_i$, where M_i and O_i are the modeled and observed values at site i, respectively. Site locations are shown in Figure S1a.

Figure 4. Spatial distribution of seasonal mean AAOD of total aerosols (left) and Aerosol Index (AI) derived from Ozone Monitoring Instrument (OMI) measurements over years of 2010–2014 (right).

Figure 5. Spatial distribution of seasonal mean near-surface concentrations of BC (μg m^{-3}) originating from the seven source regions in China (NC, SC, SW, CW, NE, NW, and TP), marked with black outlines, and sources outside China (RW). Regionally averaged BC in China contributed by individual source regions is shown at the bottom right of each panel.

Figure 6. Spatial distribution of relative contributions (%) to seasonal mean near-surface BC concentrations from each of the tagged source regions.

Figure 7. Relative contributions (%) from the tagged source regions (denoted by colors) to regional mean surface concentrations of BC over seven receptor regions in China (NC, SC, SW, CW, NE, NW, and TP) and China (seven regions combined, CN) in different seasons. The receptor regions are marked on the horizontal axis in each panel.

Figure 8. Composite differences in winds at 850 hPa (m s^{-1}) and near-surface BC concentrations (μg m^{-3}) between polluted and normal days in DJF.

Figure 9. Composite differences in surface BC concentrations (μg m^{-3}) averaged over receptor regions (marked on the horizontal axis) over eastern and central China between polluted and normal days in DJF originating from individual sources regions (bars in each column).

Figure 10. Spatial distribution of (a, b) column burden (mg m^{-2}) and (c, d) near-surface concentrations (μg m^{-3}) of BC originating from total emissions inside (CN) and outside China (RW), respectively, in March-April-May (MAM). The black solid lines over western (150°E, 20°–60°N) Pacific in panel (a) mark the cross-sections used to quantify outflow of BC from East Asia. The box over western United States (125°–105°W, 30°–50°N) in panel (c) is used to quantify BC concentrations attributed to sources from China.

Figure 11. Spatial distribution of annual mean direct radiative forcing of BC (W m^{-2}) at the top of the atmosphere originating from the tagged BC source regions in China (NC, SC, SW, CW, NE, NW, and TP) and source outside China (RW). Regionally averaged forcing in China contributed by individual source regions is shown at the bottom right of each panel.

Figure 12. (a, c) BC seasonal DRF averaged over China as a function of BC emission fraction (the ratio of regional emission to the total emission over China and global, respectively, unit: %) for each of the tagged regions. (b, d) Seasonal DRF efficiency of BC (W m^{-2} Tg^{-1}) for each of the tagged source regions over China and globally, respectively. The efficiency is defined as the DRF divided by the corresponding scaled annual emission (seasonal emission multiplied by 4). Error bars indicate 1-σ of mean values during years 2010–2014.

Figure 13. Seasonal (a, b) near-surface concentration (μg m^{-3} Tg^{-1}) and (c, d) column burden (mg m^{-2} Tg^{-1}) efficiency of BC for each of the tagged source regions over China and globally, respectively.

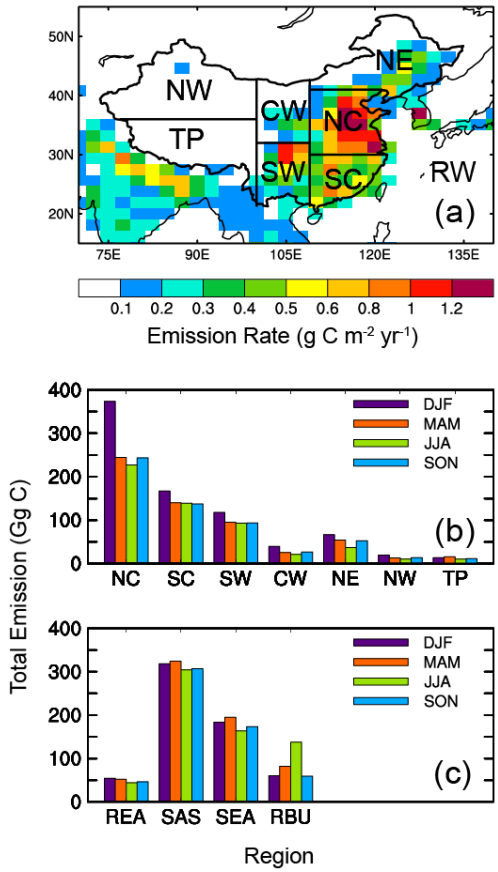

Figure 1. (a) Spatial distribution of annual mean total emissions (anthropogenic plus biomass burning, units: g C m^{-2} yr^{-1}) of black carbon (BC) averaged over 2010–2014. The geographical BC source regions are selected as North China (NC, 109°E–east boundary, 30°–41°N), South China (SC, 109°E–east boundary, south boundary–30°N), Southwest China (SW, 100°–109°N, south boundary–32°N), Central-West China (CW, 100°–109°N, 32°N–north boundary), Northeast China (NE, 109°E–east boundary, 41°N–north boundary), Northwest China (NW, west boundary–100°E, 36°N–north boundary), and Tibetan Plateau (TP, west boundary–100°E, south boundary–36°N) in China and regions outside of China (RW, rest of the world). (b) Seasonal mean total emissions (units: Gg C, Gg = 10^9g) of BC from the seven BC

source regions in China and (c) emissions from rest of East Asia (REA, with China excluded), South Asia (SAS), Southeast Asia (SEA), and Russia/Belarussia/Ukraine (RBU).

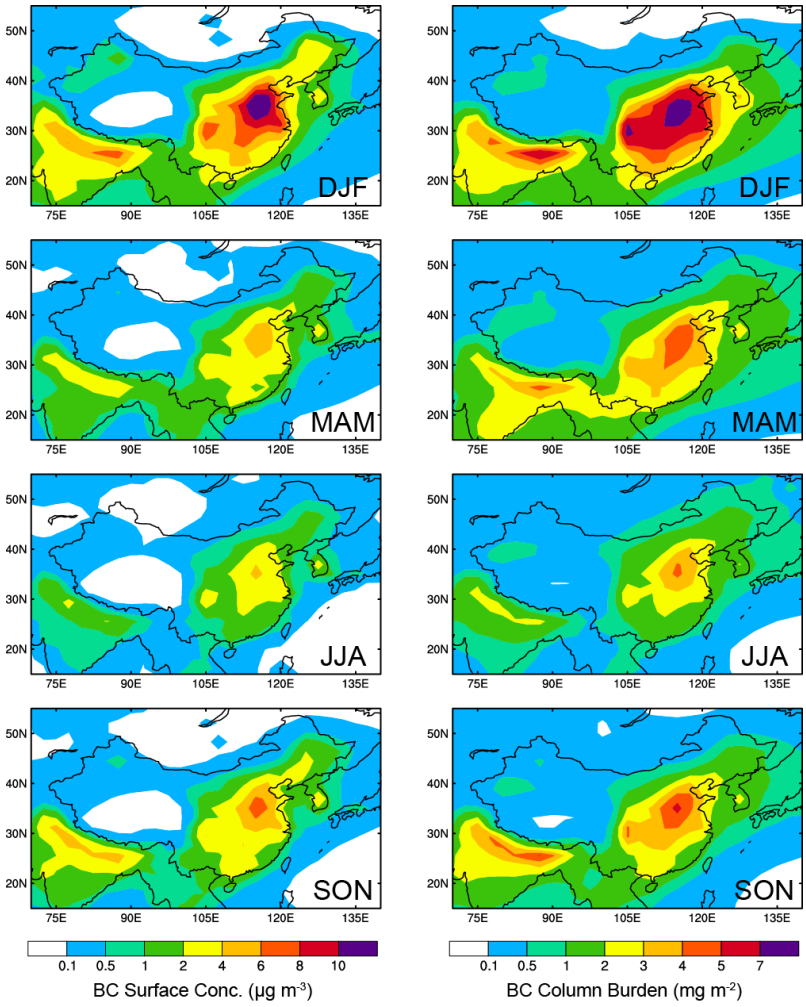

Figure 2. Simulated seasonal mean near-surface concentrations (left, units: μg m^{-3}) and column burden (right, units: mg m^{-2}) of BC in December-January-February (DJF), March-April-May (MAM), June-July-August (JJA), and September-October-November (SON).

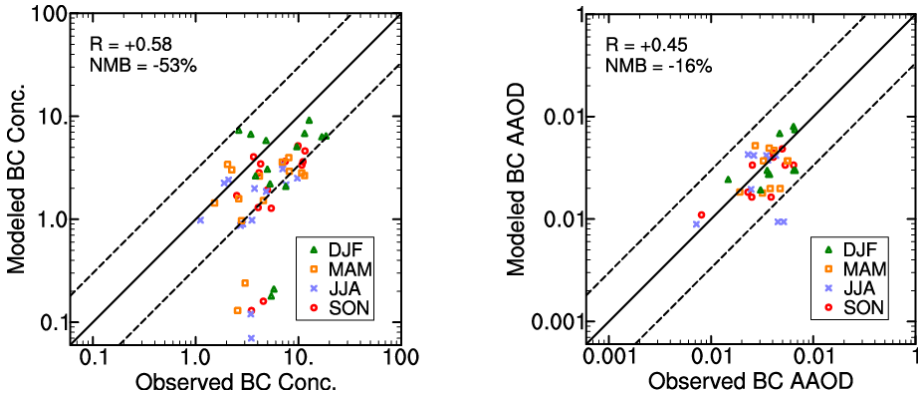

Figure 3. Comparisons of observed and modeled seasonal mean (a) near-surface concentrations (units: μg m^{-3}) and (b) aerosol absorption optical depth (AAOD) of BC in China. Solid lines mark the 1:1 ratios and dashed lines mark the 1:3 and 3:1 ratios. Observed BC concentrations were taken between 2006 and 2007 at 14 sites of the China Meteorological Administration (CMA) Atmosphere Watch Network (CAWNET) (Zhang et al., 2012). Observed AAOD of BC are obtained by removing dust AAOD from total AAOD at 10 sites of the Aerosol Robotic Network (AERONET) (Holben et al., 2001), following Bond et al. (2013). The observed AAOD are averaged over years of 2010–2014 over 7 sites and 2005–2010 over 3 sites with data available. Correlation coefficient (R) and normalized mean bias (NMB) between observation and simulation are shown on top left of each panel. NMB = $100\% \times \sum(M_i - O_i) / \sum O_i$, where M_i and O_i are the modeled and observed values at site i, respectively. Site locations are shown in Figure S1a.

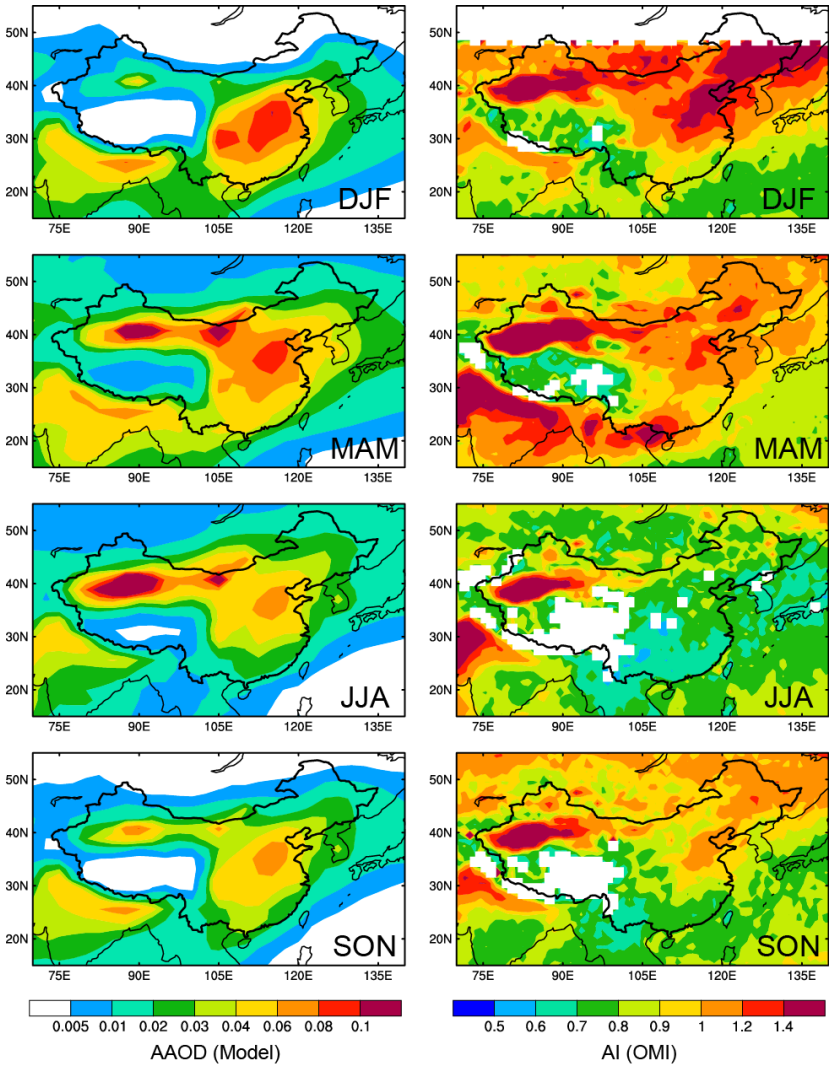

2341
2342

2343 **Figure 4.** Spatial distribution of seasonal mean AAOD of total aerosols (left) and
2344 Aerosol Index (AI) derived from Ozone Monitoring Instrument (OMI) measurements
2345 over years of 2010–2014 (right).

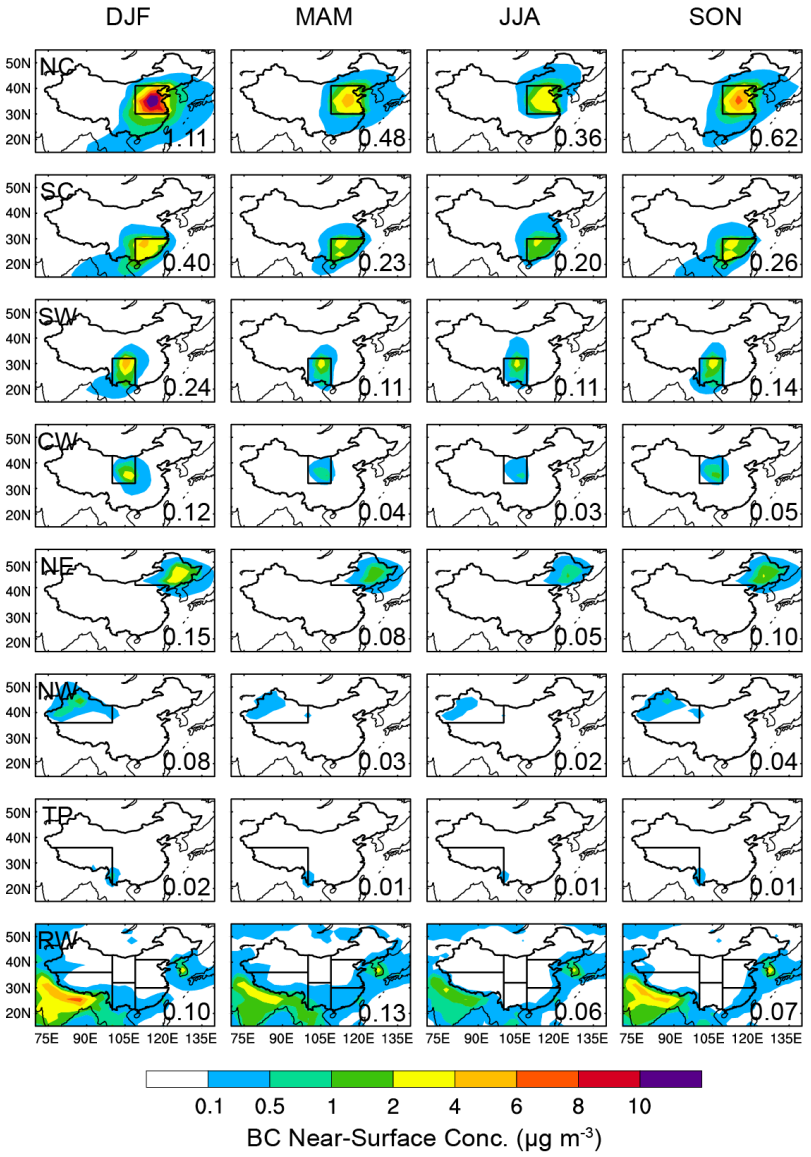

Figure 5. Spatial distribution of seasonal mean near-surface concentrations of BC (μg m^{-3}) originating from the seven source regions in China (NC, SC, SW, CW, NE, NW, and TP), marked with black outlines, and sources outside China (RW). Regionally averaged BC in China contributed by individual source regions is shown at the bottom right of each panel.

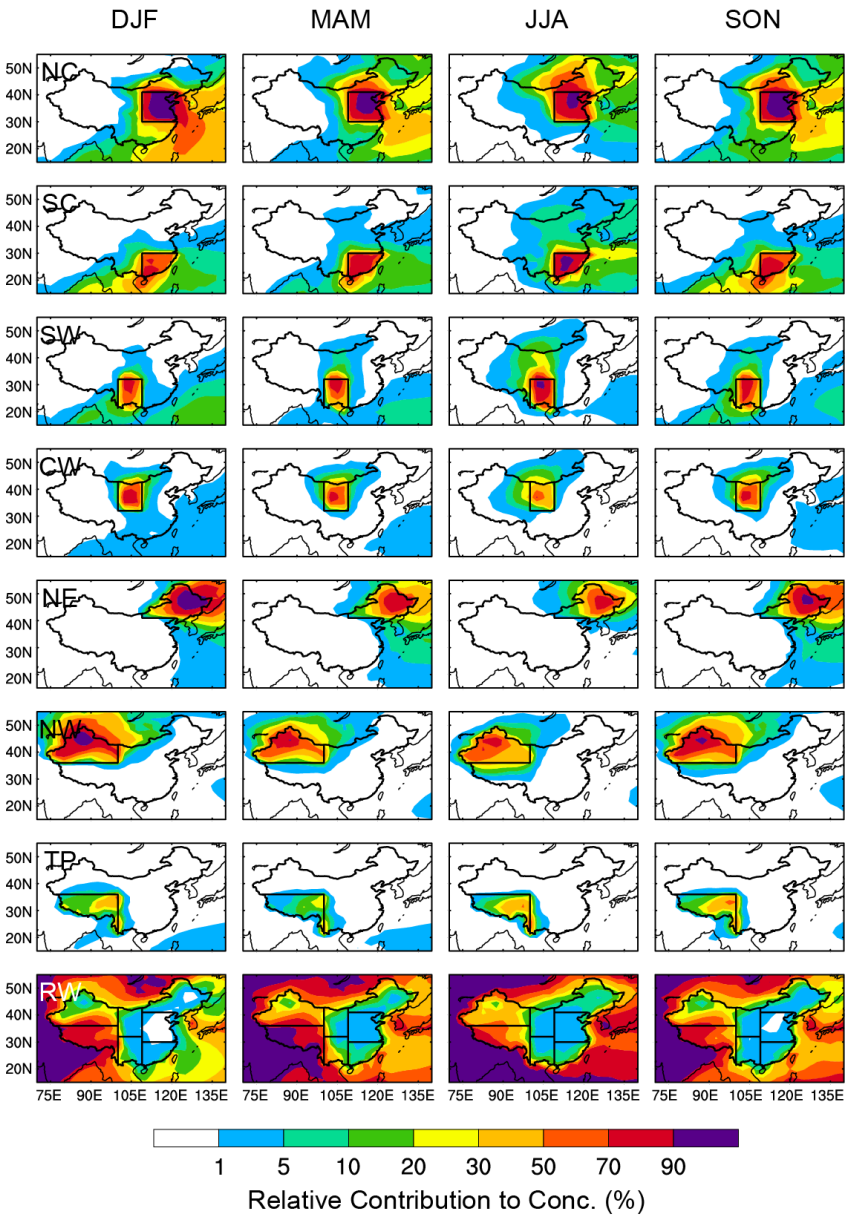

Figure 6. Spatial distribution of relative contributions (%) to seasonal mean near-surface BC concentrations from each of the tagged source regions.

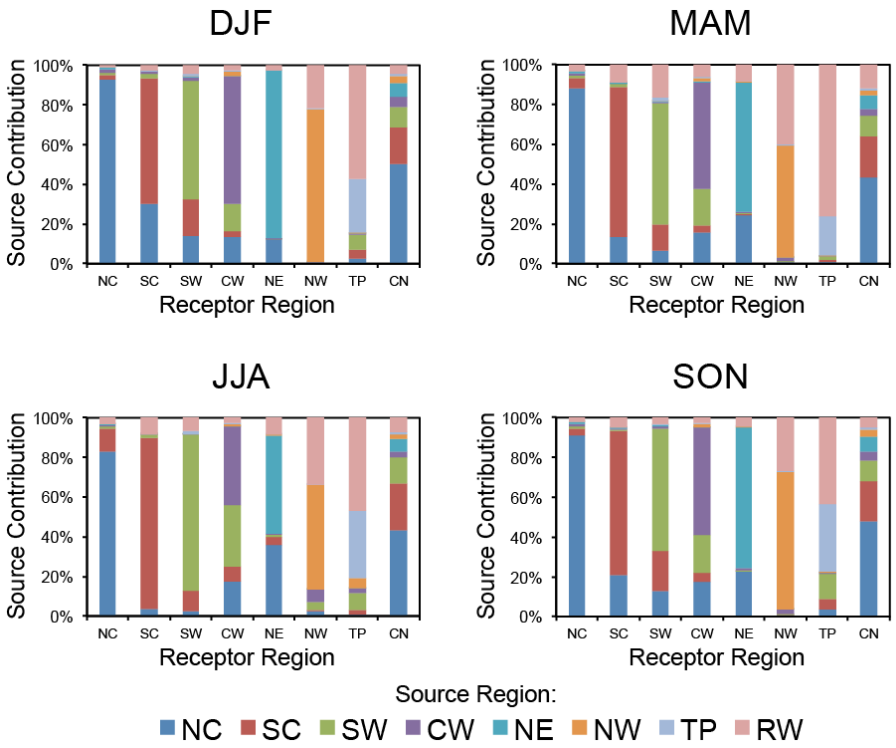

Figure 7. Relative contributions (%) from the tagged source regions (denoted by colors) to regional mean surface concentrations of BC over seven receptor regions in China (NC, SC, SW, CW, NE, NW, and TP) and China (seven regions combined, CN) in different seasons. The receptor regions are marked on the horizontal axis in each panel.

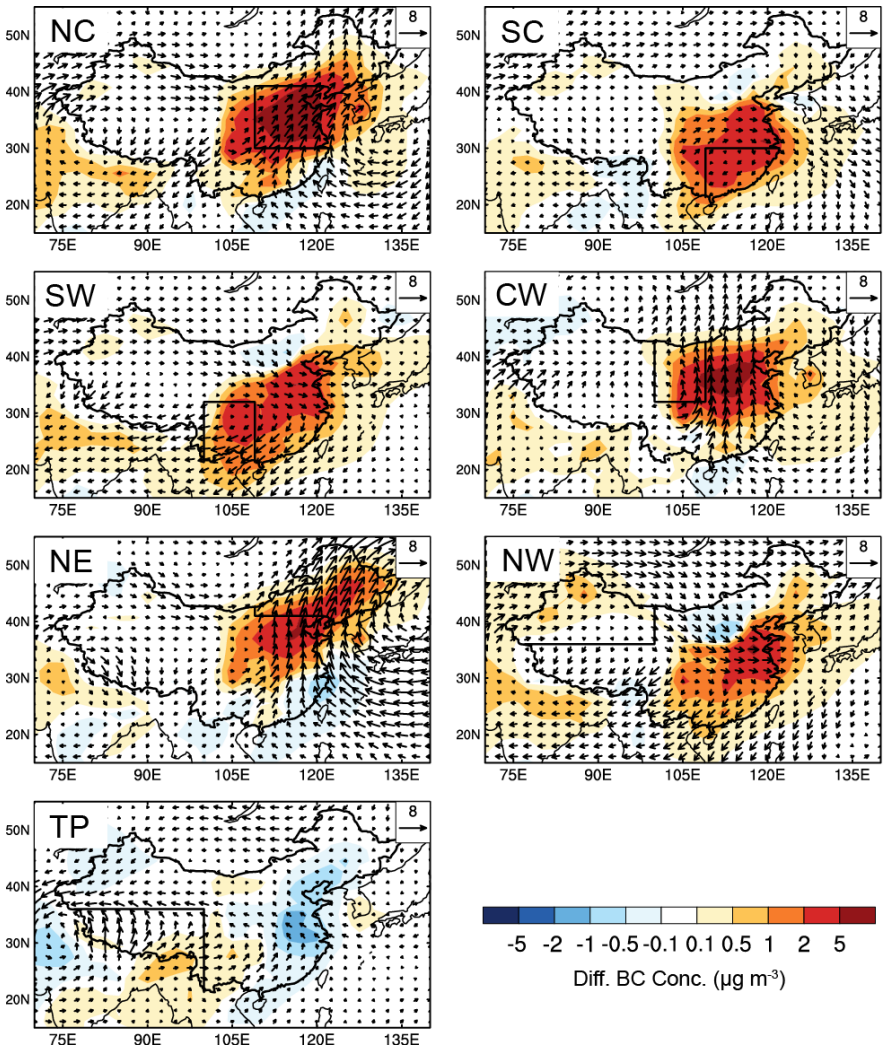

Figure 8. Composite differences in winds at 850 hPa (m s^{-1}) and near-surface BC concentrations (μg m^{-3}) between polluted and normal days in DJF.

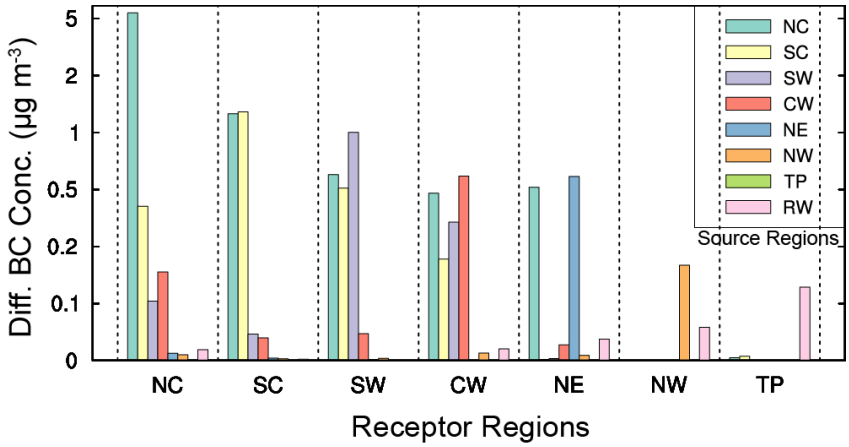

Figure 9. Composite differences in surface BC concentrations (μg m^{-3}) averaged over receptor regions (marked on the horizontal axis) over eastern and central China between polluted and normal days in DJF originating from individual sources regions (bars in each column).

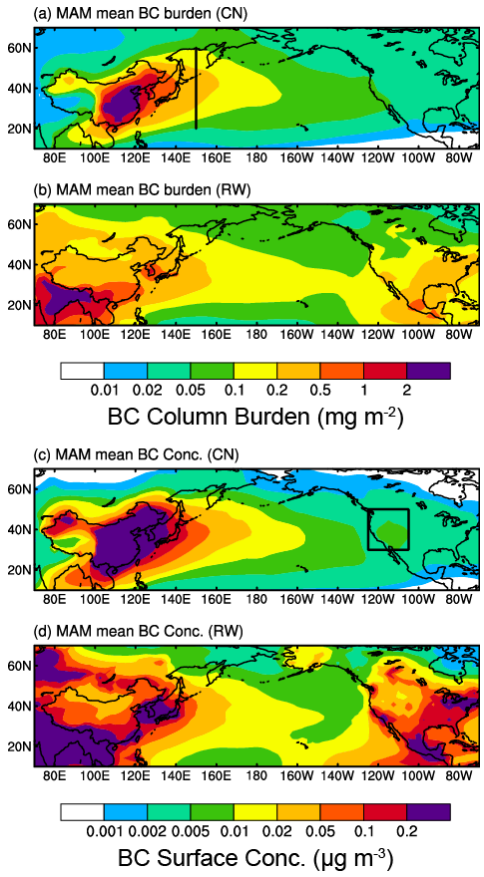

Figure 10. Spatial distribution of (a, b) column burden (mg m^{-2}) and (c, d) near-surface concentrations (μg m^{-3}) of BC originating from total emissions inside (CN) and outside China (RW), respectively, in March-April-May (MAM). The black solid lines over western (150°E, 20°–60°N) Pacific in panel (a) mark the cross-sections used to quantify outflow of BC from East Asia. The box over western United States (125°–105°W, 30°–50°N) in panel (c) is used to quantify BC concentrations attributed to sources from China.

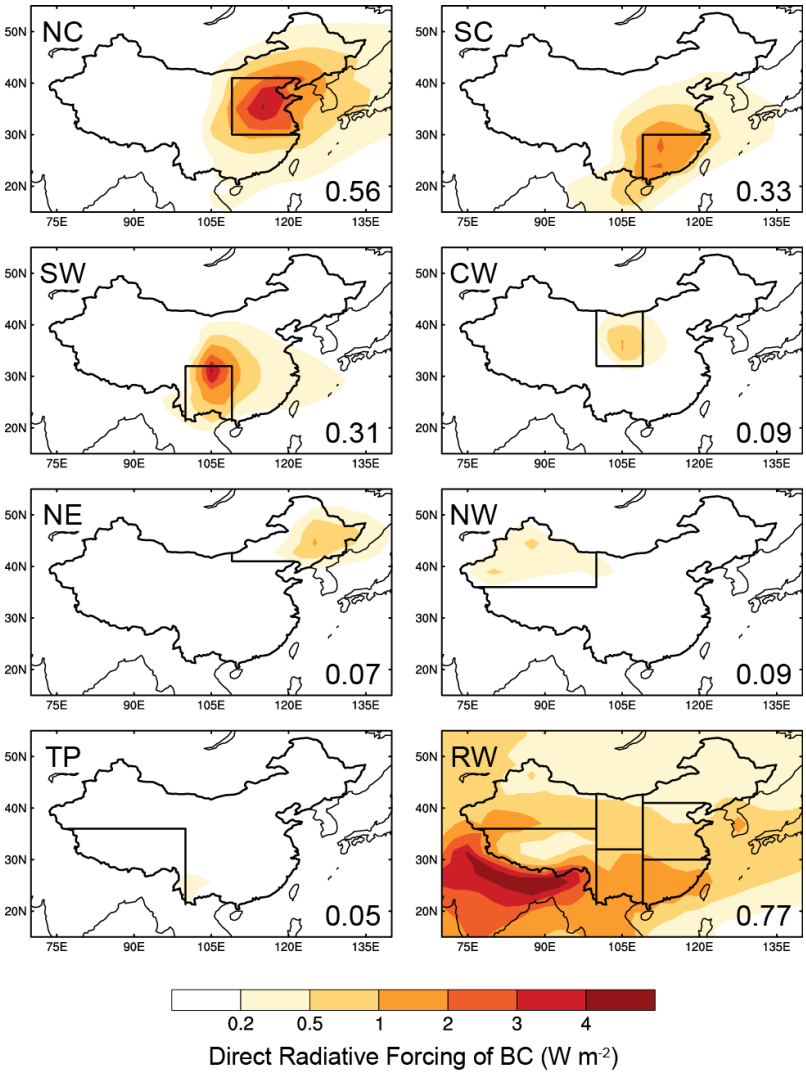

Figure 11. Spatial distribution of annual mean direct radiative forcing (DRF) of BC (W m^{-2}) at the top of the atmosphere originating from the tagged BC source regions in China (NC, SC, SW, CW, NE, NW, and TP) and source outside China (RW). Regionally averaged forcing in China contributed by individual source regions is shown at the bottom right of each panel.

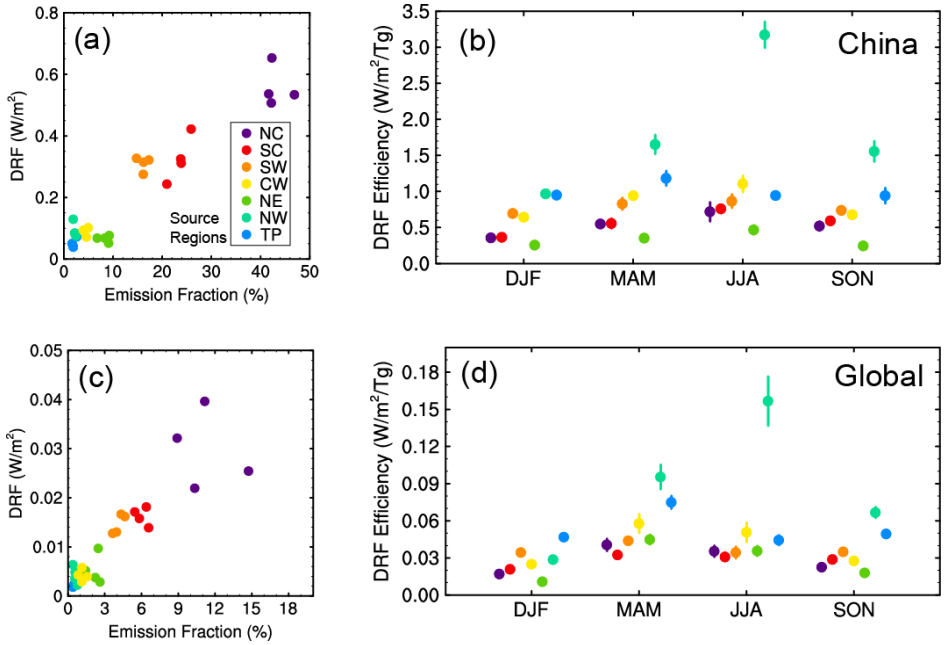

Figure 12. (a, c) BC seasonal DRF averaged over China as a function of BC emission fraction (the ratio of regional emission to the total emission over China and global, respectively, unit: %) for each of the tagged regions. (b, d) Seasonal DRF efficiency of BC (W m^{-2} Tg^{-1}) for each of the tagged source regions over China and globally, respectively. The efficiency is defined as the DRF divided by the corresponding scaled annual emission (seasonal emission multiplied by 4). Error bars indicate 1-σ of mean values during years 2010–2014.

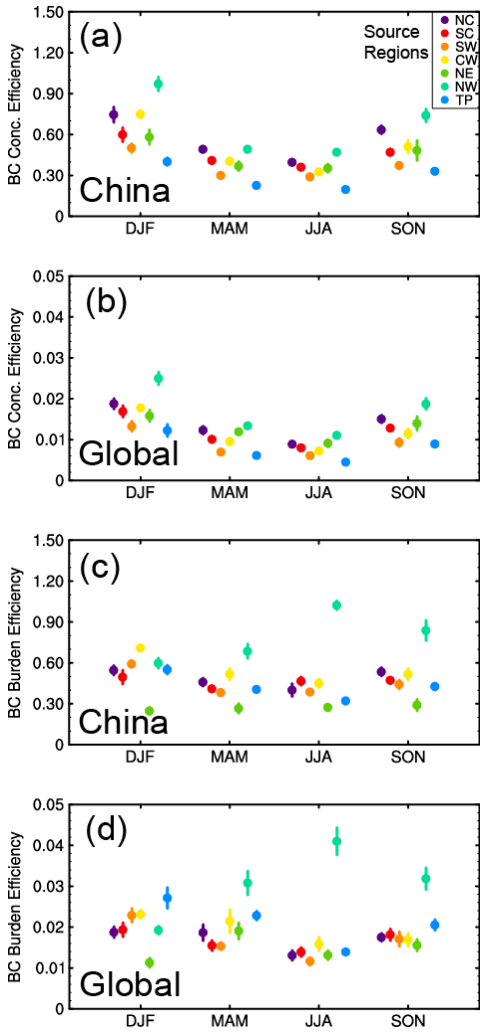

Figure 13. Seasonal (a, b) near-surface concentration (μg m^{-3} Tg^{-1}) and (c, d) column burden (mg m^{-2} Tg^{-1}) efficiency of BC for each of the tagged source regions over China and globally, respectively.